Origin of first cells at terrestrial, anoxic geothermal fields

Armen Y. Mulkidjanian[a,b,1], Andrew Yu. Bychkov[c], Daria V. Dibrova[a,d], Michael Y. Galperin[e], and Eugene V. Koonin[e,1]

[a]School of Physics, University of Osnabrück, D-49069 Osnabrück, Germany; [b]A. N. Belozersky Institute of Physico-Chemical Biology and Schools of [c]Geology and [d]Bioengineering and Bioinformatics, Moscow State University, Moscow 119992, Russia; and [e]National Center for Biotechnology Information, National Library of Medicine, National Institutes of Health, Bethesda, MD 20894

Edited* by Norman H. Sleep, Stanford University, Stanford, CA, and approved January 17, 2012 (received for review October 28, 2011)

All cells contain much more potassium, phosphate, and transition metals than modern (or reconstructed primeval) oceans, lakes, or rivers. Cells maintain ion gradients by using sophisticated, energy-dependent membrane enzymes (membrane pumps) that are embedded in elaborate ion-tight membranes. The first cells could possess neither ion-tight membranes nor membrane pumps, so the concentrations of small inorganic molecules and ions within protocells and in their environment would equilibrate. Hence, the ion composition of modern cells might reflect the inorganic ion composition of the habitats of protocells. We attempted to reconstruct the "hatcheries" of the first cells by combining geochemical analysis with phylogenomic scrutiny of the inorganic ion requirements of universal components of modern cells. These ubiquitous, and by inference primordial, proteins and functional systems show affinity to and functional requirement for K^+, Zn^{2+}, Mn^{2+}, and phosphate. Thus, protocells must have evolved in habitats with a high K^+/Na^+ ratio and relatively high concentrations of Zn, Mn, and phosphorous compounds. Geochemical reconstruction shows that the ionic composition conducive to the origin of cells could not have existed in marine settings but is compatible with emissions of vapor-dominated zones of inland geothermal systems. Under the anoxic, CO_2-dominated primordial atmosphere, the chemistry of basins at geothermal fields would resemble the internal milieu of modern cells. The precellular stages of evolution might have transpired in shallow ponds of condensed and cooled geothermal vapor that were lined with porous silicate minerals mixed with metal sulfides and enriched in K^+, Zn^{2+}, and phosphorous compounds.

prebiotic chemistry | abiotic photosynthesis | hydrothermal alteration | origin of life | Na^+/K^+ gradient

The utility of the geological record for reconstruction of the habitats of the earliest life forms is limited. Because of the heavy impact bombardment, the Earth surface underwent major changes approximately 3.8 to 3.9 Gigayears (Gyr) ago, so that only few rock samples are older than 4.0 Gyr (1, 2). Diverse recent data indicate that life might be older than the oldest known rocks (2). If life originated in the Hadean, finding any geological traces of the first life forms is unlikely.

In 1926, Archibald Macallum noted that, although similarities between seawater and organismal fluids, such as blood and lymph, indicate that the first animals emerged in the sea, the inorganic composition of the cell cytosol dramatically differs from that of modern sea water (3). Macallum insightfully pointed out that "the cell… has endowments transmitted from a past almost as remote as the origin of life on earth." Thus, in our inference of the features of the primordial organisms and their environment, we are left with the biological record which, given the evolutionary continuity, is as old as life itself. The ideas of Macallum (3) can be generalized in a "chemistry conservation principle" (4): the chemical traits of organisms are more conservative than the changing environment and hence retain information about ancient environmental conditions. Chemistry conservation is manifest, for example, in the highly reduced state of the cell interior even in those organisms that dwell in oxygenated habitats (4). The reduced state of the cytoplasm indicates that the major biochemical pathways were fixed before the atmosphere became oxygenated as a result of the activity of cyanobacteria approximately 2.4 Gyr ago (5), so that substantial modification of these pathways in response to the oxygenation of the atmosphere was impossible. Instead, cellular life forms have evolved numerous energy-requiring membrane transport systems to sustain redox and (electro)chemical gradients between their interior and the environment.

It stands to reason that simultaneous consideration of various boundary conditions has the potential to eliminate most of the vast number of scenarios for the early evolution of life that appear possible in principle (4). Under this premise, we have previously addressed diverse facets of the early life problem from the viewpoint of photochemistry (6), comparative genomics (7–9), and energetics (10, 11). The principle of chemistry conservation can be used as an additional major constraint for reconstructing primordial environmental conditions in the absence of reliable geological record. For example, ancient, ubiquitous proteins often use Zn and Mn, but not Fe, as transition metal cofactors; this preference is retained across the three domains of life (12). The abundance of Zn- and Mn-dependent enzymes during the earliest steps of evolution and the later recruitment of Fe has been inferred also from a global phylogenomic reconstruction (13). The prevalence of Zn-dependent ancestral enzymes is particularly remarkable given the low estimated concentration of Zn in the anoxic ocean of 10^{-12} to 10^{-16} M (14, 15) and indicates that the first organisms might have dwelled in specific, Zn-enriched habitats (12, 16).

Here we combine geochemical evidence with the data on the overall ionic composition of the modern cells, with a particular emphasis on their universal preference for K^+ ions over Na^+ ions. Geochemical analysis shows that, contrary to the common belief that associates the origin of life with marine environments, the first cells could have emerged at inland geothermal fields within ponds of condensed and cooled geothermal vapor. Conceptually, this scenario of early evolution resembles Darwin's "warm little pond" vision (17).[†] Under this scenario, the ocean

Author contributions: A.Y.M. designed research; A.Y.M., A.Y.B., D.V.D., M.Y.G., and E.V.K. performed research; A.Y.M., A.Y.B., and E.V.K. contributed new reagents/analytic tools; A.Y.M., A.Y.B., D.V.D., M.Y.G., and E.V.K. analyzed data; and A.Y.M., A.Y.B., D.V.D., M.Y.G., and E.V.K. wrote the paper.

The authors declare no conflict of interest.

Freely available online through the PNAS open access option.

*This Direct Submission article had a prearranged editor.

[1]To whom correspondence may be addressed. E-mail: amulkid@uos.de or koonin@ncbi.nlm.nih.gov.

This article contains supporting information online at www.pnas.org/lookup/suppl/doi:10.1073/pnas.1117774109/-/DCSupplemental.

[†]"But if (and oh what a big if) we could conceive in some warm little pond with all sorts of ammonia and phosphoric salts, light, heat, electricity &c. present, that a protein compound was chemically formed, ready to undergo still more complex changes…." —from Darwin's 1871 letter to Joseph Hooker (17).

was invaded by life at a later stage, following the emergence of ion-tight phospholipid membranes.

Results and Discussion

Inorganic Ion Requirements of Ubiquitous Cellular Systems. The total intracellular content of an ion reflects the ability of the cell to accumulate this ion against the concentration gradient. In particular, Table 1 shows that concentrations of K^+, Zn^{2+}, phosphate, and several other inorganic ions in all cells are orders of magnitude higher than the levels of these ions in modern sea water, as well as in the primordial, anoxic ocean. Conversely, the content of Na^+ ions in the cells is much lower than it is in the sea water. Many halophiles that can tolerate high external levels of NaCl increase the internal K^+ concentration up to approximately 1.0 M, to keep the internal K^+/Na^+ ratio high (18). Apparently, it is not so much the actual concentrations of K^+ and Na^+ but the K^+/Na^+ ratio of at least 1 that is critical for the proper functioning of the cell.

Modern cells can maintain the ionic disequilibria because their membranes are ion-tight and contain a plethora of membrane-embedded, energy-dependent ion-translocating protein complexes (i.e., ion pumps). Accordingly, cells invest large amounts of energy into sustaining the respective ion gradients. For example, neurons, even in the resting state, use approximately 20% of their ATP to maintain the K^+/Na^+ gradient across the membrane (19).

Under the chemistry conservation principle, the striking difference between the intracellular inorganic chemistry and the composition of sea water suggests that the first cellular organisms dwelled in specific habitats that were enriched for the elements that are prevalent in modern cells (3, 4, 12, 16, 20). A potential alternative to this explanation is that the chemical differences between the intracellular milieu and the environment are unrelated to the conditions under which the first cells evolved (21). Then, the dramatic enrichment of modern cells for K^+, Zn^{2+}, and phosphate could be viewed as a relatively late shift that came after the emergence of powerful ion-translocating membrane pumps and was driven by the growing demand of the newly evolving enzymes for particular inorganic ions as catalysts or substrates.

To distinguish between these two explanations, we turned to the proteins that are shared by (nearly) all cellular organisms with sequenced genomes and by inference originate from the so-called last universal cellular (or common) ancestor (LUCA) or an even earlier stage of evolution (7, 22–27). The ion preferences of the ubiquitous, ancient proteins are expected to provide information about the habitats of the first cells. Indeed, the ion-tight membranes of modern cells are extremely complex energy conversion and transport systems that obviously are products of long evolution and could not possibly exist in the first protocells. According to the available reconstructions, the first lipids were simple and single-tailed (28–31). The experiments with such lipids compounds have shown that vesicles made of fatty acids (28, 32) or of phosphorylated isoprenoids (33) can reliably entrap polynucleotides and proteins. Such membranes, however, are leaky to small molecules (30, 32). Hence, the membranes of first cells probably could occlude biological polymers and even facilitate their transmembrane translocation but could not prevent (almost) free exchange of small molecules and ions with the environment. Furthermore, before the emergence of diverse membrane translocators, the exchange of small molecules via leaky membranes should have been of vital importance for the first cells, which also implies that their interior was equilibrated with the surroundings, at least with respect to small molecules and ions (30, 32, 34–38).

SI Appendix, Table S1, lists the ion requirements and affinities of the ubiquitous proteins that represent the heritage of the LUCA and probably of protocells (7, 27). Besides the preference for Zn and Mn, which has been discussed previously (12, 16), several proteins and functional systems that can be traced back to the LUCA—and probably beyond—require K^+, whereas none of the surveyed ancestral proteins specifically requires Na^+. The majority of the (nearly) universal proteins that can be confidently traced to the LUCA are involved in translation, which is potassium-dependent both in bacteria (39) and in archaea (40, 41). Potassium seems to be required for at least two essential ribosomal reactions. First, K^+ ions are needed for the peptidyl transferase center to assume its functional conformation (42). Second, our sequence and structure comparisons indicate that the key translation factors are K^+-dependent GTPases (*SI Appendix*, Figs. S1–S4 and Table S2 provide further details).

Phylogenetic analysis of GTPases shows that extensive diversification of GTPase domains antedated the LUCA (43). The K^+-binding sites are highly conserved in diverse GTPases, indicating that they were already present in the primordial GTPase domains (*SI Appendix*). Perhaps even more telling are reconstructions showing that the peptidyl transferase center is the core, ancestral part of the ribosome (44, 45). Thus, the K^+-dependent components of the translation system appear to stem from the protocell (or even earlier) stage of evolution. Apparently, the dominance of K^+ over Na^+ in modern cells, which is reverse to the case in sea water, was important also for the protocells.

The concentration of phosphate in the cytosol is at least four orders of magnitude greater than in the sea water (Table 1). Not surprisingly, the energetics of the protocells, which can be inferred from the inspection of the ubiquitous protein set, must have been based on phosphate transfer reactions and specifically

Table 1. Approximate concentrations of key ions in various environments

Ion, mol/L	Modern sea water	Anoxic water of primordial ocean	Cell cytoplasm
Na^+	0.4	>0.4	0.01
K^+	0.01	~0.01	0.1
Ca^{2+}	0.01	~0.01	0.001
Mg^{2+}	0.05	~0.01	0.01
Fe	10^{-8} (mostly Fe^{3+})	10^{-5}	10^{-3} to 10^{-4}
Mn^{2+}	10^{-8}	10^{-6} to 10^{-8}	10^{-6}
Zn^{2+}	10^{-9}	$<10^{-12}$	10^{-3} to 10^{-4}
Cu	10^{-9} (Cu^{2+})	$<10^{-20}$ (Cu^{1+})	10^{-5}
Cl^-	0.5	>0.1	0.1
PO_4^{3-}	10^{-6} to 10^{-9}	$<10^{-5}$	~10^{-2} (mostly bound)

The intracellular concentration is defined here as the total content of a particular element divided by the cell volume and should be discriminated from the much lower free ion concentration, which does not account for the ions that are bound to biological molecules. The reconstructed chemical composition of the anoxic ocean includes data from refs. 14, 15, 58, 141. The data on intracellular concentrations of different chemical elements are based on refs. 14, 142–145.

on hydrolysis of nucleoside triphosphates (*SI Appendix*, Table S1). That phosphate-based metabolism is ancestral in cellular life follows also from the results of the recent global phylogenomic analysis (13). Given that the backbones of nucleic acids contain phosphate groups, there is no doubt that phosphate was a central component of life from its inception.

However, the concentration of phosphate ions in natural aqueous systems, such as lakes or seas, could never be as high as it is inside cells because of the poor solubility of Ca and Mg phosphates. Thus, although the requirement for a high phosphate concentration in the protocells is indisputable, it remains unclear how the protocells could accumulate phosphate without tight membranes and phosphate-scavenging pumps. It has been argued that more reduced phosphorous compounds such as hypophosphite (PO_2^{3-}) and/or phosphite (PO_3^{3-}), which are approximately 1,000 times more soluble than phosphate, could have been abundant under primordial reduced conditions (46–49).

Hence a major conundrum:

a) Intracellular concentrations of key ions, in particular K^+, Zn^{2+}, and phosphate, are several orders of magnitude higher compared with sea water, both extant and that of Hadean ocean (according to the available reconstruction; Table 1);
b) (Nearly) universal, and by inference primordial, proteins and functional systems show affinity to and functional requirement for K^+, Mg^{2+}, Zn^{2+}, Mn^{2+}, and phosphate, but not Na^+ (*SI Appendix*, Table S1); and
c) It is extremely unlikely that protocells possessed ion-tight membranes with built-in ion pumps.

Given these observations and inferences, it appears most likely that protocells evolved in habitats characterized by a high K^+/Na^+ ratio and relatively high concentrations of Zn^{2+}, Mn^{2+} and phosphorous compounds.

Vapor-Dominated Zones of Terrestrial Geothermal Systems as Possible Hatcheries of First Cells. Is it possible to envision any natural habitats with high levels of transition metals and phosphorous compounds, as well as a K^+/Na^+ ratio substantially greater than 1?

As argued previously (10–12), high concentrations of transition metals, such as Zn and Mn, are found only where extremely hot hydrothermal fluids leach metal ions from the crust and bring them to the surface. Such thermal systems operate either on the sea floor (50, 51), or at sites of continental (i.e., terrestrial) geothermal activity where the metal ions are carried not only by hot fluids, but also by steam (52, 53).

Phosphate concentrations are low both in the sea water (Table 1) and in the fluids of the deep sea hydrothermal vents (~0.5 μM) (50). The content of phosphorous compounds is higher in terrestrial thermal springs, where it varies within a broad range, reaching 60 to 70 μM in some Yellowstone springs (54) and as much as 1 mM in the acidic mud pots of Kamchatka (55). In an attempt to discriminate phosphite from phosphate in field samples, Pech et al. have found comparable amounts of phosphate and phosphite in a pristine geothermal pool at Hot Creek Gorge near Mammoth Lakes, CA, which is fed by hot, bicarbonate-rich geothermal waters (56). The discovery of highly soluble phosphite in a modern geothermal pool can at least partly account for high amounts of phosphorus in the discharges of terrestrial geothermal systems. Furthermore, this finding could explain why diverse prokaryotes possess systems of hypophosphite and phosphite oxidation (57).

The high K^+/Na^+ ratio should be taken as the key search criterion because accumulation of transitional metals or phosphorous compounds is conceivable in primordial evaporating water basins; evaporation, however, cannot affect the K^+/Na^+ ratio. No marine environment with a K^+/Na^+ ratio greater than 1 has ever been described or reconstructed to our knowledge. In trapped samples of Archaean seawater, the K^+/Na^+ ratio is approximately 0.025 and is similar to that in modern oceans (58). Arguably, this low K^+/Na^+ ratio was established in the ocean shortly after its formation, when it was still too hot to be compatible with life (2, 58). The K^+/Na^+ ratio is similarly low in hydrothermal fluids of marine hot vents because these vents are fed predominantly by sea water (50).

Terrestrial aqueous systems, which are mostly fed by water from rain and snow, are more variable with respect to the K^+/Na^+ ratios. Generally, the concentrations of K^+ and Na^+ ions in rivers and lakes are much less than 1 mM, and the K^+/Na^+ ratio is in the range of 0.1 to 1.0, although in streams that interact with potassium-rich igneous rocks, this ratio can reach 2 or 3 (59, 60). At sites of inland geothermal activity, the levels of K^+ and Na^+ are higher as a result of extensive leaching of metals from rocks by hot, carbonate-enriched waters, and the K^+/Na^+ ratio varies within a broad range (54, 55) owing to the intrinsic heterogeneity of such systems. The heterogeneity is a result of the boiling of the ascending hot hydrothermal fluids at shallower depths followed by separation of the vapor phase from the liquid phase (Fig. 1). Upon separation, gaseous compounds, such as H_2S, CO_2, and NH_3, redistribute into vapor that rises upward toward the surface. The subsurface area in which steam and gas prevail in open fractures is called the vapor-dominated zone (Fig. 1). The exhalations from vapor-dominated zones, which are enriched in

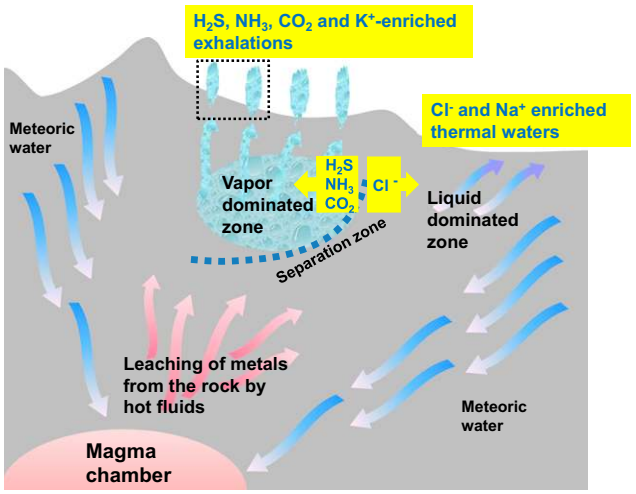

Fig. 1. A terrestrial geothermal system (scheme based on refs. 52, 53, 62, 138) that is fed mostly by water from rain and snow (meteoric water) which, when it is deep underground, mixes with cation- and anion-enriched magmatic fluids and becomes heated to 300 to 500 °C; such hot fluids can leach diverse ions from the hot rock. Upon heating, the water becomes lighter and, being enriched in metal cations and such anions as Cl^-, HS^-, and CO_3^{2-}, ascends toward the surface. At shallower depths, the rising hot water starts to boil because of lower pressure. The vapor phase usually separates from the liquid phase, which leads to the typical zoning (53, 62). The separation is not only physical but also chemical; e.g., whereas Cl^- anions mostly stay in the liquid phase, the gaseous compounds, such as CO_2, NH_3, and H_2S, redistribute into vapor. The flow route of the liquid phase and the exact point of its discharge are determined by the crevices within the rock; the ejected fluids are characterized by slightly alkaline pH and high content of chloride and sodium, which both can be traced to the contribution of magmatic waters. The vapor rises upward and spreads within the rock; the subsurface area that is filled by steam and gas is called the vapor-dominated zone. Part of the steam condenses near the surface and is ejected by the thermal springs, and the rest of the steam reaches the surface through fissures of the rock to form fumaroles (i.e., steam vents). Metal cations are carried both by the liquid and by the vapor phases (52, 53), although the K^+/Na^+ ratio is higher in the vapor phase (Table 2).

H_2S, CO_2, NH_3 and metal cations, discharge as steam (i.e., fumaroles) or, after condensation, as mud pots (*SI Appendix*, Fig. S5) because of the silica that is also carried by the vapor (52–55, 61, 62). Numerous fumaroles and mud pots overlaying a vapor-dominated zone make a geothermal field.

The emissions from the vapor-dominated zones of inland geothermal systems are K^+-enriched, unlike the discharges from the liquid-dominated zones, which contain much more Na^+ than K^+ (54, 55). To our knowledge, the causes of this enrichment have not been explicitly addressed. Comparison of the concentrations of some essential elements in the fluids of thermal springs and in the vapor of the same springs (Table 2 shows data from Kamchatka volcanic system) sheds light on the probable mechanisms of K^+ enrichment. As follows from the data in Table 2, the K^+/Na^+ ratio is, on average, higher in the vapor condensate than in the liquid. A similar dependence can be inferred from data on the two largest vapor-dominated geothermal fields of modern Earth: at the Larderello geothermal field in Italy, the K^+/Na^+ ratio reached 32 in the steam condensate (63), whereas the steam condensates at The Geysers geothermal field in California showed a K^+/Na^+ ratio as high as 75 (64). Thus, the high K^+/Na^+ ratios in the exhalations from the vapor-dominated zones of inland hydrothermal systems could be a result of the higher volatility of K^+ ions within the vapor phase; the larger K^+ ions are expected to more readily form complexes with such molecules as H_2O, H_2S, or CO_2 and anions.

Thus, among the well characterized environments on Earth, only emissions from vapor-dominated zones of inland geothermal systems simultaneously show K^+/Na^+ ratios much greater than 1, a high content of transition metals, and substantial levels of phosphorous compounds (Table 2) (55, 62, 63, 65). Although terrestrial geothermal systems have been occasionally suggested as potential habitats of the early life (37, 61, 66), the unique role of their vapor-dominated zones as natural chemical separators, to our knowledge, has not been specifically addressed. The principal reason why the vapor-dominated fields were not considered as suitable hatcheries for the protocells is that the fluids at such fields are highly acidic [with pH values reaching −0.5 (54, 55); Table 2] and hence inhospitable to life. However, acidity appears to be a characteristic of modern geothermal fields but not the primordial ones. Indeed, the ascending vapor carries large amounts of hydrogen sulfide, which, when it reaches the surface, is oxidized by atmospheric oxygen to strong sulfuric acid. In the absence of oxygen on the primordial Earth, the geochemistry of vapor-dominated geothermal fields should have been quite different:

a) The pH of the discharges from the vapor-dominated zones should have been closer to neutral because both H_2S and CO_2, which ascend with the vapor, are weak acids, and their acidity is usually compensated by the interaction with basic rocks;
b) At neutral pH, silica would precipitate at the outlets of thermal springs and around them not as amorphous kaolinite/mud, as it does now (61), but as porous, ordered silicate minerals. Thus, the formation of clays such as smectite/montmorillonite and illite, as well as zeolites such as laumontite and natrolite, should be expected;
c) In the absence of oxygen, sulfide ions would cause precipitation of metal sulfides, as is the case at modern deep-sea hydrothermal systems, where slowly precipitating ZnS particles form halos around the vent throats which are built of fast-precipitating sulfides of iron and copper (50, 51). At ancient geothermal fields, because of the high silica content in the

Table 2. Concentration of some essential elements in the water of thermal springs and in the condensate of the same springs

	Spring Number					
Element	S6–14	S6–15	S6–16	S6–17	S6–18	S6–19
	Water composition, parts per billion					
t, °C	94.00	93.00	89.00	93.00	96.00	96.00
pH	0.50	−0.28	0.25	−0.58	−0.09	−0.30
B	95,109	54,142	35,927	72,639	83,813	133,910
Ca	279,893	121,911	455,703	213,657	334,430	168,640
Fe	384,075	174,308	245,163	258,688	446,416	250,982
K	89,606	138,879	22,881	882,720	86,835	155,190
Mg	168,491	68,883	118,968	78,648	202,059	98,071
Mn	7,355	2,909	3,358	3,942	9,424	4,325
Na	128,609	100,599	79,224	479,027	143,699	121,597
Ni	140	89	82	96	593	67
P	7,399	8,615	6,434	33,689	7,568	9,163
Ti	9,170	2,345	2,300	3,106	8,533	7,874
Zn	657	324	734	471	830	439
	Condensate composition, parts per billion					
pH	2.29	2.19	2.54	2.03	1.05	2.03
B	2,635.0	84.4	1,092.3	184.6	214.6	4,295.5
Ca	566.7	219.2	424.4	30.0	90.0	288.9
Fe	760.4	216.3	798.5	10.7	154.6	99.4
K	15,787.2	45.5	2,317.2	22.6	37.6	8,398.6
Mg	141.0	48.7	138.9	2.5	15.5	24.5
Mn	9.0	2.3	7.0	0.1	1.9	2.3
Na	5,427.1	127.8	797.6	14.9	50.7	3,082.5
Ni	16.2	0.4	9.2	0.2	1.3	0.7
P	18.0	5.2	11.8	2.0	6.6	4.3
Ti	18.7	16.6	8.3	0.5	2.6	4.1
Zn	19.0	3.4	12.8	6.0	6.9	10.8

For Mutnovsky volcano, Kamchatka peninsula, see *Methods* and refs. 62, 95.

exhalations of the vapor-dominated systems, the formation of metal-sulfide–contaminated clays and zeolites rather than pure metal-sulfide precipitates should be expected.

It is generally believed that the primordial atmosphere was CO_2-dominated and that the atmospheric pressure was higher than it is now (67, 68). Both these factors would boost the transportation of diverse ions by the ascending vapor. The high CO_2 concentration would enhance the leaching from the rock by carbonate ions, whereas the high atmospheric pressure would bring the boiling isotherm (Fig. 1) closer to the surface, shorten the distance that had to be covered by the ascending vapor, and thereby increase the amount of transported inorganic ions.

In summary, the operation of geothermal systems under anoxic, CO_2-dominated atmosphere would result in vigorous discharge of neutral geothermal fluids and steam from their vapor-dominated zones; the discharges would have a K^+/Na^+ ratio greater than 1 and would be enriched in NH_3, H_2S, CO_2, phosphorous compounds, and transition metals. These terrestrial geothermal fields appear to provide the best environment on the primordial Earth for the origin of protocells.

Evolution of Protocells at Anoxic Geothermal Fields. Fig. 2 shows a scenario for the origin of protocells at anoxic geothermal fields overlaying the vapor-dominated zone of a primordial geothermal system (as detailed in the legend to Fig. 2). Such systems should have been typical of the first Earth continent(s) that are believed to have formed from Mg-, K-rich ultramafic rocks (2, 69). The analysis of the 4.02- to 4.19-Gyr–old inclusion-bearing zircons indicates an early presence of subduction zones and, hence, the overlying geothermal fields (70). In the absence of oxygen, the transition metals would precipitate mostly as sulfides. While ZnS and MnS precipitate slowly, Cu_2S, PbS, and FeS_2 are promptly removed by precipitation at neutral pH and at temperatures lower than 300 °C (71–73). Therefore, Cu_2S, PbS, and FeS_2 could not spread far away from points of discharge, especially taking into account the cooling of the geothermal fluids to the ambient temperatures. In addition, Zn is much more volatile than Fe, as could be judged from the analyses of geothermal springs (Table 2) and volcanic vapor (74). Hence, far-off ponds and puddles, fed by cooled geothermal fluids and condensed vapor, would have been particularly enriched in slowly precipitating Zn^{2+} and Mn^{2+} ions, with their beds covered by clays and zeolites contaminated by sulfides and carbonates of Zn and Mn (Fig. 2*A*). We hypothesize that such loose, Zn- and Mn-enriched sediments served as the cradles for protocells (Fig. 2*B*). The affinity of many ubiquitous proteins for Zn^{2+} and, to a lesser extent, Mn^{2+} (*SI Appendix*, Table S1) implies that these proteins might have evolved in such environments.

The absence of any enzymes related to autotrophy in the ubiquitous protein set (*SI Appendix*, Table S1) suggests that the protocells were heterotrophs, i.e., their growth depended on the supply of abiotically produced organic compounds (32, 75–77). At least two continuous, abiotic sources of such compounds would exist in the described geothermal systems. First, even in modern vapor-dominated geothermal systems, exhalations carry organic molecules that are believed to be formed, at least partly, in the process of hydrothermal alteration of ultramafic rocks (78, 79). Hydrothermal alteration occurs when iron-containing rocks interact with water at temperatures of approximately 300 °C, which is typical of terrestrial geothermal systems. Under these conditions, part of the Fe^{2+} in the rock is oxidized to Fe^{3+}, yielding magnetite (Fe_3O_4). The electrons released through this reaction are accepted by protons of water yielding H_2; in the presence of water-dissolved CO_2, diverse hydrocarbons are ultimately produced (78). It could be argued that the hydrothermal rock alteration might also account for the reduction of insoluble apatite to soluble phosphite (47), explaining the presence of phosphite in the geothermal fluids (56). Similar reactions could lead to the ammonia formation (80), which might account for the high ammonia content in the exhalations of geothermal fields [as much as 130 mg/L in the mud pot solutions of Kamchatka (55)]. In addition, diverse organic molecules could be produced by abiotic photosynthesis catalyzed by ZnS and MnS particles (81–84). Such crystals are semiconductors, which can trap quanta with a λ of less than 320 nm and transiently store their energy in a form of charge-separated states, capable of reducing diverse compounds at the surface (81). Thereby, crystals of ZnS are the most powerful photocatalysts known in nature (10).[‡] Particles of ZnS can catalyze photopolymerization reactions (85) and photoreduce carbonaceous compounds to diverse organic molecules, including intermediates of the tricarboxylic acid cycle (83, 84); the highest quantum yield of 80% was observed upon reduction of CO_2 to formate (81).

Generally, two types of environments relevant for the early stages of evolution can be discriminated at primordial geothermal fields: (*i*) periodically wetted and illuminated mineral surfaces that could serve as templates and catalysts for diverse abiotic syntheses and (*ii*) geothermal pools that could serve as hatcheries of first replicating life forms (Fig. 2). At mineral surfaces of primordial geothermal fields, ammonia, sulfide, phosphite, and phosphate ions would react with carbonaceous compounds, yielding aminated, sulfurated, and phosphorylated molecules (48, 49), which could provide nourishment and fuel

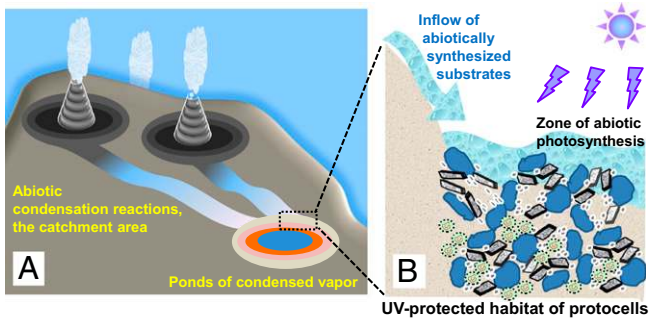

Fig. 2. Evolution of protocells at a primordial anoxic geothermal field. (*A*) Anoxic geothermal field over a terrestrial geothermal system; the figure corresponds to the boxed section in Fig. 1. A primordial geothermal system could form over a "hot spot," similar to modern Island (139) or a primitive subduction zone (52, 69, 70, 140). The cooling of the ascending, H_2S-enriched vapor causes precipitation of metal sulfides, particularly pyrite, which starts beyond the surface. At the point of water/vapor discharge, H_2S starts to escape into the atmosphere, thus increasing the pH of the discharging fluids. By analogy with modern geothermal fields, the geothermal fluids and condensed vapor are expected to run down the slope, cool down and loose transition metals through sulfide precipitation. At neutral pH, Cu_2S, PbS, and FeS_2, shown by dark colors, should have precipitated first (71–73), leaving Mn and Zn ions in the liquid phase. The relief depressions gave rise to lakes, ponds or puddles; at a certain distance from the thermal springs, after the cooling of geothermal fluids and the fall-out of Cu_2S, PbS, and FeS_2, these basins should have became particularly enriched in Zn^{2+} and Mn^{2+} ions, with their beds covered by ZnS and MnS-containing silicate minerals (shown by yellow color). (*B*) An anoxic geothermal pond as a sink for diverse (organic) substrates delivered by geothermal fluids and abiotically (photo)synthesized at minerals. These substrates could be consumed by protocells that are shown dwelling in the deeper, UV protected layers of the pond bed, within inorganic compartments build of silica minerals and metal sulfide particles.

[‡]ZnS, broadly known as phosphor (from "phosphorescence"), shows a unique ability to convert diverse kinds of energy, including that of light quanta, X-rays, electrons (as in displays), α-particles (ZnS was introduced as the first inorganic scintillator by Sir William Crookes in 1903), into (electro)chemical energy of separated electric charges (reviewed in ref. 10).

for the protocells within the geothermal ponds. Each such pool would "harvest," with the help of geothermal streams and rain water, substrates from its catchment area. Only water-soluble compounds or compounds that could be carried by water (e.g., as micelles of amphiphilic molecules) could reach such ponds. This harvesting mechanism essentially excludes the interference of "tar," which would inevitably form under conditions of abiotic syntheses (4), with the chemistry within geothermal ponds.

In the absence of an ozone shield, the protocells would need protection from the UV component of solar light (86). Both ZnS and MnS crystals efficiently scavenge UV up to approximately 320 nm (81, 87). The molar absorption coefficient of ZnS particles is approximately 2 mM cm^{-1} at 260 nm, at which nucleotides absorb (88). It is easy to estimate that a thin, 5-μm layer of ZnS would attenuate the UV light by a factor of 10^{10}. Thus, even conservatively assuming a 90% porosity of ZnS-containing sediments and a 1% ZnS content in the sediments, a 5-mm layer of ZnS-containing precipitates would give the same UV protection as a greater than 100 m water column (cf. ref. 86). This is a low bound estimate because other mineral constituents of siliceous sediments would also absorb UV and protect the primordial life forms (89). Hence, a stratified system could be established within geothermal ponds, where the illuminated upper layers would be involved in the "harvesting" and production of reduced organic compounds, whereas the deeper, less productive but better protected layers could provide shelter for the protocells (Fig. 2*B*). The porosity of the silica minerals would enable metabolite transport between the layers. Both the light gradient and the interlayer metabolite exchange are typical of modern stratified phototrophic microbial communities (90).

Thus, Hadean anoxic geothermal fields would provide:

(a) Water basins with ionic composition compatible with that of modern cells, meeting the chemistry conservation criterion;
(b) A supply of organic molecules that could fuel biosynthetic reactions;
(c) Abundant, efficient, and versatile (photo)catalysts, above all ZnS and Zn^{2+} ions;
(d) Microcompartments within porous, siliceous ZnS- and MnS-containing masses.

The proposed scenario is robust because its critical parameters, such as the K^+/Na^+ ratio greater than 1 and the continuous supply of reduced compounds, are sustained by multiple complementary mechanisms. In particular, the high K^+ levels and the K^+/Na^+ ratio greater than 1 would have been maintained by the K-enrichment of the primordial igneous rocks (2), by the higher mobility of K^+ ions in the vapor phase (Table 2), and by ability of 2:1 clay minerals, such as smectites and illite, to select potassium over sodium (91). The only vital parameter for the model is the absence of atmospheric oxygen, which is not disputed when it comes to the first eons of Earth history (5, 67).

Furthermore, geothermal fields have autonomous heat sources and good thermal isolation provided by the air, so the temperature and chemical composition of water basins in these habitats are defined primarily by the geothermal activity and are effectively independent of the climate, potentially allowing protocells to endure climate changes or even periods of early glaciations (67). Taken together, these considerations seem to make inland anoxic geothermal fields the best incubators for the protocells among all currently known habitats on Earth.

Terrestrial Anoxic Geothermal Fields as Cradles for Earliest Life Forms? So far, we have focused on the conditions under which the protocells might have evolved, without addressing the earlier steps of evolution. Comparison of extant genomes does not directly yield information on pre-LUCA life forms. However, features of these primordial organisms can be gleaned from the analysis of those protein families that were represented in the LUCA by multiple paralogues such as GTPases or aminoacyl-tRNA synthetases (92) (*SI Appendix*, Table S1). Most likely, the ancestors of these protein families shared the ionic requirements of the extant family members, such as those for K^+ and Zn^{2+}. A similar preference for Zn^{2+}, Mn^{2+}, and ATP as substrate is shown by viral hallmark genes (*SI Appendix*, Table S3). These genes encode proteins which are present in many viral families but are absent from cellular organisms and could stem from organisms that preceded the LUCA (9, 93). Thus, extending the chemistry conservation principle, we hypothesize that terrestrial geothermal fields, similar to those illustrated in Fig. 2*A*, might have also served as the cradles of life itself, sheltering the first, precellular life forms up to the stage of the LUCA. This scenario seems to be compatible with several lines of evidence:

a) Remaining almost independent of the ambient climate, inland geothermal fields could exist for millions of years, long enough to serve as incubators not only for the protocells but also for the preceding life forms.
b) The major biochemical building blocks are derivatives of those molecules that preferably partition to the vapor phase upon the geothermal separation, namely simple carbonaceous and phosphorous compounds, ammonia, and sulfide. In addition, the vapor phase of geothermal systems is particularly enriched in borate, the concentration of which can reach 10 mM (Table 2) (54, 94, 95) and which seems to be important for the stabilization of ribose (96, 97).
c) Geothermal fields should have offered ample opportunity for the reagents to concentrate and interact upon evaporation. Specifically, the wetted surfaces would undergo continuous drying resulting in selective accumulation of the least volatile compounds, which, in this case, would be simple amides, with boiling points of approximately 200 °C due to their ability to form strong hydrogen bonds. Formamide, the likely key building block for abiotic synthesis of nucleotides and amino acids (98–108), could form via hydrolysis of hydrogen cyanide, which is found in volcanic gases and in exhalations of geothermal fields (109). In addition, elimination of a water molecule from ammonia salts of carboxylic acids could also yield amides, in particular, formamide from ammonia formate. As noted earlier, exhalations of geothermal fields contain high amounts of ammonia (55); part of this ammonia is of non-sedimentary origin (110) and could have been present already in the primordial geothermal vapor. Formate and other carboxylic acids would also have been produced at anoxic geothermal fields (as detailed earlier). Hence, anoxic geothermal fields could selectively accumulate simple amides, primarily formamide, most likely mixed with water and other simple molecules in different ratios. The yield of photochemical and thermal syntheses in amide-containing solutions could be further enhanced by catalytic action of mineral surfaces. Specifically, it has been shown that silica minerals catalyze the formation of adenine and cytosine from formamide (103, 111) and that TiO_2, the main component of the mineral rutile, could catalyze the formation not only of purine derivatives but also of thymine, 5-hydroxymethyluracil, and even acyclonucleosides (112). Even widespread iron oxides have been shown to catalyze the synthesis of nucleobases from formamide (113).
d) Spontaneous polymerization events, which are thermodynamically unfavorable in the bulk water, would be favored at geothermal fields. Strikingly, a thermodynamic "window" at concentrations of formamide of greater than 30% has been identified, at which polynucleotides were more stable than mononucleotides (114, 115). In addition, condensation reactions would be favored by the wet/dry cycles driven by the intrinsic pulsation of thermal springs (66), daily oscillations

of temperature and light, and the capacity of silicate minerals to serve as apt templates (116–118).

e) The exceptional photostability of biological nucleotides suggests that they could have been selected under solar UV radiation from a plethora of diverse abiotically (photo) synthesized organic compounds (6, 119–122). Analogously, photoselection might have facilitated the transition from complex mixtures of small organic molecules to the "RNA world" (123) by favoring photostable RNA-like polymers with excitonically coupled, stacked nucleotides forming Watson–Crick pairs (6, 119, 124). In addition, solar UV radiation could support primeval syntheses not only by catalyzing photopolymerization, but also by breaking the less photostable organic molecules and thus supplying building blocks for new synthetic cycles (10).

f) Under the low luminosity of the young sun (67), the daily temperature oscillations could lead to periodic freezing events, favoring the concentration of reactants, the endurance of RNA-like oligomers, and their pairing (37).

g) The Zn^{2+} and Mn^{2+} ions could shape the primeval biochemistry as selective catalysts and as stabilizers of nascent biopolymers (10, 12). It has been shown that Zn^{2+}, to a much greater extent than any other transition metal ion, favored the formation of naturally occurring 3′–5′ phosphodiester bonds during abiotic polymerization of activated nucleotides (125).

h) Last but not least, evolution of life from the very first RNA-like molecules to the stage of protocells in the same habitats is the most parsimonious scenario: otherwise, one would have to envision mechanisms for relocation of the first precellular organisms to geothermal fields from some other location and their accommodation in new habitats.

Protocells Could Not Emerge in Marine Habitat: Late Escape of Life to the Ocean. Apparently, no marine environment could ever provide a K^+/Na^+ ratio of greater than 1 or concentrate phosphate up to its level in the cells. Thus, our analysis argues against the widespread belief that the first cells evolved in marine habitats. Although early evolutionary scenarios usually considered shallow seawaters where solar light was available as an energy source (116, 126), deep-sea environments have been invoked later, initially because of the protection against the hazards of the solar UV that the water column would provide to the primordial life forms. In particular, it has been estimated that the UV component should have been attenuated by a factor as high as 10^9 to avoid irreparable damage to the first organisms (86). Russell and coworkers have noticed that FeS/FeS_2 precipitates around hydrothermal vents form expansive honeycomb-like structures and suggested that such iron-sulfide "bubbles" could encase and protect the first life forms before the emergence of cells with modern-type membranes (127, 128). Subsequently, attention has been drawn to low-temperature vents where the hydrothermal fluids are enriched in diverse organic compounds that are formed through serpentinization, a hydrothermal alteration process that is typical of the basaltic oceanic crust (129).

The terrestrial scenario outlined here incorporates all the features of the hydrothermal vents that favor the origin and early evolution of life, and adds more (Table P1 in Summary). Our scenario includes production of organic molecules from CO_2 not only in reactions of hydrothermal alteration within the rocks but also via abiotic photosynthesis at the surface. The UV protection by ZnS, MnS, and silicate minerals is much more efficient than the protection by a water column. Continental geothermal fields are even more compartmentalized than marine hydrothermal systems. Not only do they include microcompartments, such as variably hydrated pores within ZnS and MnS-containing silicate minerals, but in addition, each pond or puddle can be itself considered a separately evolving macrocompartment; occasional exchange of genetic material between these macrocompartments could be triggered by rains or overflowing of the geothermal fields.

Detailed analysis of the transition from the first biomolecules to the first cells is beyond the scope of this work; it is nevertheless clear that this transition should have been accompanied by selection for increasingly tighter cellular envelopes (36–38). Increasing sequestering of primordial life forms should have followed the evolution of their metabolic pathways (36, 130) and also would protect the informational systems from external hazards (10, 12).

The dramatic difference between the ionic compositions of the cytosol and seawater (Table 1) implies that cellular organisms could invade the ocean only after the emergence of ion-tight membranes. These membranes and the appropriate ion pumps were required to maintain the intracellular chemical environment similar to that in which the protocells evolved. Being encased by ion-tight membranes and endowed with ion pumps, the first cells could invade terrestrial water basins with low K^+/Na^+ ratios and then, via rivers, reach the ocean, where they would have been severely challenged by the high sodium levels. Therefore, they would require ion pumps capable of ejecting Na^+ ions out of the cell against large concentration backpressure. As argued previously on the basis of phylogenomic analysis of rotary ATPases, the interplay between several Na^+ pumps might have led to the emergence of membrane bioenergetics, initially in its ancestral, Na^+-using form (38, 131, 132).

The proposed terrestrial origin of the first cells implies that life started not as a planetary but as a local event, confined to a long-lasting inland geothermal field or to a network of such fields at a continental volcanic system. Only the invasion of the ocean by membrane-encased organisms transformed life into a planetary phenomenon.

Conclusions

Building on the geochemical data and the results of phylogenomic analysis, we argue here that anoxic geothermal fields overlaying the vapor-dominated zones of terrestrial hydrothermal/volcanic systems could be the most suitable hatcheries for the protocells and, most likely, the preceding replicator systems. These putative cradles of life share all of the advantages of the deep sea hydrothermal vents that have been previously proposed in the same capacity (127–129), including the presence of inorganic compartments, versatile catalysts, and sources of organic matter (Table P1 in Summary). In addition, and in contrast to deep sea vents, terrestrial geothermal fields are conducive to condensation reactions and enable the involvement of solar light as an energy source and a selective factor that would favor the accumulation of nucleotides, which are particularly photostable (6, 121, 124). Also in contrast to deep sea vents, the geothermal vapor is enriched in phosphorous and boron compounds (Table 2) that could be essential for the emergence of first RNA-like oligomers (96, 97).

Reconstruction of conditions under which the first life forms might have emerged is important for experimental modeling of the origin of life (32, 37). Some of the most successful attempts to simulate primitive abiogenic reactions have been conducted under conditions that are compatible with reconstructed conditions at the geothermal fields of the anoxic Earth. These promising experiments include syntheses of biologically relevant compounds in formamide solutions (98–108, 111–115), photosynthesis/photoselection of natural nucleotides (120–122, 133), montmorillonite-catalyzed formation of long RNA oligomers (118) and membrane vesicles (134), RNA polymerization in the eutectic phase in water–ice (135), abiotic UV photosynthesis of the tricarboxylic acid cycle intermediates at ZnS (83, 84) and TiO_2 crystals (136), as well as UV-triggered recharging of ADP to ATP (137). Further experimental exploration of models that mimic the conditions at anoxic geothermal fields are expected to shed more light on precellular evolution.

Methods

Steam samples were collected by using a specially constructed condensing device that aimed to minimize the possible contamination from the drops of liquid phase or incomplete condensation of vapors. The thermal spring (i.e., mud pot) was covered by a vapor collector that contained a refractor to prevent the eventual contamination by drops of liquid (*SI Appendix*, Fig. S6) (95). The temperature was controlled by a temperature sensor; the difference between the temperature in the vent and at the wall of the collector did not exceed 1 °C. The collector was connected to a glass Allihn condenser (i.e., bulb condenser). The condenser was continuously cooled by cold water from a tank. The vapor flow was regulated by changing the placement of the vapor collector. The sampling conditions were chosen in such a way that the temperature of the condensate outflow did not exceed 30 °C. Accordingly, if the vapor flow was too strong, the condenser was elevated so part of the steam could escape around the edges of the collector (*SI Appendix*, Fig. S6). After installation at a steam vent, the collector was equilibrated for 10 min. After that, the samples were gathered in several 50-mL vials (at least two per spring) during 2 h to ensure the reproducibility of results. When checked afterward, the concentration difference between samples obtained from the same spring did not exceed 10%, whereas the concentration differences between the samples taken from different springs could vary by orders of magnitude (Table 2). The samples of the liquid phase of the same thermal springs were filtered at the spot by using 0.45-μM membrane filters. All samples were preserved by the addition of HNO_3 up to a final concentration of 3%. The samples were later analyzed by inductively coupled plasma MS by using an Element2 (Finnegan) mass spectrometer.

ACKNOWLEDGMENTS. Valuable discussions with Drs. D. A. Cherepanov, M. Eigen, R. M. Hazen, G. F. Joyce, M. J. van Kranendonk, V. N. Kompaninchenko, D.-H. Lankenau, D. L. Pinti, M. J. Russell, V. P. Skulachev, H.-J. Steinhoff, J. Szostak, N. E. Voskoboynikova, R. J. P. Williams, Y. I. Wolf and A. Yonath are greatly appreciated. The authors are thankful to Drs. A. S. Karyagina and I. Y. Nikolaeva for providing photographs of boiling mud pots. This study was supported by Deutsche Forschungsgemeinschaft (DFG) Grants DFG-Mu-1285/1-10 and DFG-436-RUS 113/963/0-1 (to A.Y.M.), Russian Government Grant 02.740.11.5228 (to A.Y.M.), the Volkswagen Foundation (A.Y.M.), EU COST CM0902 Action (A.Y.M.), Deutscher Akademischer Austausch Dienst (D.V.D.), Russian Foundation for Basic Research Grants 10-05-00320 (to A.Y.B.) and 0-04-91331 (to D.V.D.), and the Intramural Research Program of the National Library of Medicine at the National Institutes of Health (M.Y.G. and E.V.K).

1. Nisbet EG, Sleep NH (2001) The habitat and nature of early life. *Nature* 409: 1083–1091.
2. Sleep NH (2010) The Hadean-Archaean environment. *Cold Spring Harb Perspect Biol* 2:a002527.
3. Macallum AB (1926) The paleochemistry of the body fluids and tissues. *Physiol Rev* 6: 316–357.
4. Mulkidjanian AY, Galperin MY (2007) Physico-chemical and evolutionary constraints for the formation and selection of first biopolymers: Towards the consensus paradigm of the abiogenic origin of life. *Chem Biodivers* 4:2003–2015.
5. Hazen RM, et al. (2011) Needs and opportunities in mineral evolution research. *Am Mineral* 96:953–963.
6. Mulkidjanian AY, Cherepanov DA, Galperin MY (2003) Survival of the fittest before the beginning of life: Selection of the first oligonucleotide-like polymers by UV light. *BMC Evol Biol* 3:12.
7. Koonin EV (2003) Comparative genomics, minimal gene-sets and the last universal common ancestor. *Nat Rev Microbiol* 1:127–136.
8. Koonin EV, Martin W (2005) On the origin of genomes and cells within inorganic compartments. *Trends Genet* 21:647–654.
9. Koonin EV (2009) On the origin of cells and viruses: Primordial virus world scenario. *Ann N Y Acad Sci* 1178:47–64.
10. Mulkidjanian AY (2009) On the origin of life in the zinc world: 1. Photosynthesizing, porous edifices built of hydrothermally precipitated zinc sulfide as cradles of life on Earth. *Biol Direct* 4:26.
11. Mulkidjanian AY (2011) Energetics of the first life. *Origins of Life: The Primal Self-Organization*, eds Egel E, Lankenau D-H, Mulkidjanian AY (Springer Verlag, Heidelberg), pp 3–33.
12. Mulkidjanian AY, Galperin MY (2009) On the origin of life in the zinc world. 2. Validation of the hypothesis on the photosynthesizing zinc sulfide edifices as cradles of life on Earth. *Biol Direct* 4:27.
13. David LA, Alm EJ (2011) Rapid evolutionary innovation during an Archaean genetic expansion. *Nature* 469:93–96.
14. Williams RJP, Frausto da Silva JJR (2006) *The Chemistry of Evolution: The Development of Our Ecosystem* (Elsevier, Amsterdam).
15. Anbar AD (2008) Oceans. Elements and evolution. *Science* 322:1481–1483.
16. Mulkidjanian AY, Galperin MY (2010) On the abundance of zinc in the evolutionarily old protein domains. *Proc Natl Acad Sci USA* 107:E137.
17. Darwin C (1887) *The Life and Letters of Charles Darwin, Including an Autobiographical Chapter* (John Murray, London).
18. Roberts MF (2004) Osmoadaptation and osmoregulation in archaea: Update 2004. *Front Biosci* 9:1999–2019.
19. Silver IA, Erecińska M (1997) Energetic demands of the Na^+/K^+ ATPase in mammalian astrocytes. *Glia* 21:35–45.
20. Natochin YV (2007) The physiological evolution of animals: Sodium is the clue to resolving contradictions. *Herald Russ Acad Sci* 77:581–591.
21. Dupont CL, Butcher A, Valas RE, Bourne PE, Caetano-Anollés G (2010) History of biological metal utilization inferred through phylogenomic analysis of protein structures. *Proc Natl Acad Sci USA* 107:10567–10572.
22. Gogarten JP, et al. (1989) Evolution of the vacuolar H^+-ATPase: Implications for the origin of eukaryotes. *Proc Natl Acad Sci USA* 86:6661–6665.
23. Doolittle WF, Brown JR (1994) Tempo, mode, the progenote, and the universal root. *Proc Natl Acad Sci USA* 91:6721–6728.
24. Woese C (1998) The universal ancestor. *Proc Natl Acad Sci USA* 95:6854–6859.
25. Lazcano A, Forterre P (1999) The molecular search for the last common ancestor. *J Mol Evol* 49:411–412.
26. Philippe H, Forterre P (1999) The rooting of the universal tree of life is not reliable. *J Mol Evol* 49:509–523.
27. Charlebois RL, Doolittle WF (2004) Computing prokaryotic gene ubiquity: Rescuing the core from extinction. *Genome Res* 14:2469–2477.
28. Deamer DW, Dworkin JP (2005) Chemistry and physics of primitive membranes. *Top Curr Chem* 259:1–27.
29. Gotoh M, et al. (2007) Possible molecular evolution of biomembranes: From single-chain to double-chain lipids. *Chem Biodivers* 4:837–848.
30. Deamer DW (2008) Origins of life: How leaky were primitive cells? *Nature* 454:37–38.
31. Mulkidjanian AY, Galperin MY (2010) Evolutionary origins of membrane proteins. *Structural Bioinformatics of Membrane Proteins*, ed Frishman D (Springer, Heidelberg), pp 1–28.
32. Mansy SS, et al. (2008) Template-directed synthesis of a genetic polymer in a model protocell. *Nature* 454:122–125.
33. Nomura SM, et al. (2001) Towards proto-cells: "Primitive" lipid vesicles encapsulating giant DNA and its histone complex. *ChemBioChem* 2:457–459.
34. Deamer DW (1997) The first living systems: A bioenergetic perspective. *Microbiol Mol Biol Rev* 61:239–261.
35. Szostak JW, Bartel DP, Luisi PL (2001) Synthesizing life. *Nature* 409:387–390.
36. Szathmáry E (2007) Coevolution of metabolic networks and membranes: The scenario of progressive sequestration. *Philos Trans R Soc Lond B Biol Sci* 362: 1781–1787.
37. Ricardo A, Szostak JW (2009) Origin of life on earth. *Sci Am* 301:54–61.
38. Mulkidjanian AY, Galperin MY, Koonin EV (2009) Co-evolution of primordial membranes and membrane proteins. *Trends Biochem Sci* 34:206–215.
39. Conway TW (1964) On the role of ammonium or potassium ion in amino acid polymerization. *Proc Natl Acad Sci USA* 51:1216–1220.
40. Bayley ST, Kushner DJ (1964) The ribosomes of the extremely halophilic bacterium, *Halobacterium cutirubrum*. *J Mol Biol* 9:654–669.
41. Yonath A (2002) The search and its outcome: High-resolution structures of ribosomal particles from mesophilic, thermophilic, and halophilic bacteria at various functional states. *Annu Rev Biophys Biomol Struct* 31:257–273.
42. Miskin R, Zamir A, Elson D (1970) Inactivation and reactivation of ribosomal subunits: The peptidyl transferase activity of the 50 s subunit of *Escherichia coli*. *J Mol Biol* 54: 355–378.
43. Leipe DD, Wolf YI, Koonin EV, Aravind L (2002) Classification and evolution of P-loop GTPases and related ATPases. *J Mol Biol* 317:41–72.
44. Bokov K, Steinberg SV (2009) A hierarchical model for evolution of 23S ribosomal RNA. *Nature* 457:977–980.
45. Davidovich C, Belousoff M, Bashan A, Yonath A (2009) The evolving ribosome: From non-coded peptide bond formation to sophisticated translation machinery. *Res Microbiol* 160:487–492.
46. Gulick A (1955) Phosphorus as a factor in the origin of life. *Am Sci* 43:479–489.
47. Hanrahan G, Salmassi TM, Khachikian CS, Foster KL (2005) Reduced inorganic phosphorus in the natural environment: Significance, speciation and determination. *Talanta* 66:435–444.
48. Schwartz AW (2006) Phosphorus in prebiotic chemistry. *Philos Trans R Soc Lond B Biol Sci* 361:1743–1749.
49. Pasek MA, Kee TP, Bryant DE, Pavlov AA, Lunine JI (2008) Production of potentially prebiotic condensed phosphates by phosphorus redox chemistry. *Angew Chem Int Ed Engl* 47:7918–7920.
50. Kelley DS, Baross JA, Delaney JR (2002) Volcanoes, fluids, and life at mid-ocean ridge spreading centers. *Annu Rev Earth Planet Sci* 30:385–491.
51. Tivey MK (2007) Generation of seafloor hydrothermal vent fluids and associated mineral deposits. *Oceanography (Wash DC)* 20:50–65.
52. Hedenquist JW, Lowenstern JB (1994) The role of magmas in the formation of hydrothermal ore-deposits. *Nature* 370:519–527.
53. Williams-Jones AE, Heinrich CA (2005) Vapor transport of metals and the formation of magmatic-hydrothermal ore deposits. *Econ Geol* 100:1287–1312.
54. Fournier RO (2004) *Geochemistry and Dynamics of the Yellowstone National Park Hydrothermal System* (US Geological Survey, Menlo Park, CA).
55. Bortnikova SB, Gavrilenko GM, Bessonova EP, Lapukhov AS (2009) The hydrogeochemistry of thermal springs on Mutnovskii Volcano, southern Kamchatka. *J Volcanology and Seismology* 3:388–404.
56. Pech H, et al. (2009) Detection of geothermal phosphite using high-performance liquid chromatography. *Environ Sci Technol* 43:7671–7675.

57. White AK, Metcalf WW (2007) Microbial metabolism of reduced phosphorus compounds. *Annu Rev Microbiol* 61:379–400.
58. Pinti DL (2005) The origin and evolution of the oceans. *Lectures in Astrobiology*, eds Gargaud M, Barbier B, Martin H, Reisse J (Springer-Verlag, Berlin), pp 83–111.
59. Hem JD (1985) *Study and Interpretation of the Chemical Characteristics of Natural Water. U.S Geological Survey Water-Supply Paper 2254* (US Government Printing Office, Washington, DC), 3rd Ed.
60. Drever JI (1997) *The Geochemistry of Natural Waters: Surface and Groundwater Environments* (Prentice Hall, Englewood Cliffs, NJ), 3rd Ed.
61. Deamer D, Singaram S, Rajamani S, Kompanichenko V, Guggenheim S (2006) Self-assembly processes in the prebiotic environment. *Philos Trans R Soc Lond B Biol Sci* 361:1809–1818.
62. Bychkov AY (2009) *Geochemical Model of Present-Day Ore Formation in the Uzon Caldera* (GEOS, Moscow).
63. Duchi V, Minissale A, Manganelli M (1992) Chemical composition of natural deep and shallow hydrothermal fluids in the Larderello geothermal field. *J Volcanol Geotherm Res* 49:313–328.
64. Bouwer H (1979) Geothermal power production with irrigation waste water. *Ground Water* 17:375–384.
65. Karpov GA, Naboko SI (1990) Metal contents of recent thermal waters, mineral precipitates and hydrothermal alteration in active geothermal fields, Kamchatka. *J Geochem Explor* 36:57–71.
66. Kompanichenko VN (2009) Changeable hydrothermal media as potential cradle of life on a planet. *Planet Space Sci* 57:468–476.
67. Kasting JF, Catling D (2003) Evolution of a habitable planet. *Annu Rev Astron Astrophys* 41:429–463.
68. Sleep NH, Bird DK, Pope EC (2011) Serpentinite and the dawn of life. *Philos Trans R Soc Lond B Biol Sci* 366:2857–2869.
69. Van Kranendonk MJ (2010) Two types of archean continental crust: Plume and plate tectonics on early Earth. *Am J Sci* 310:1187–1209.
70. Hopkins M, Harrison TM, Manning CE (2008) Low heat flow inferred from >4 Gyr zircons suggests Hadean plate boundary interactions. *Nature* 456:493–496.
71. Seewald JS, Seyfried WE (1990) The effect of temperature on metal mobility in subseafloor hydrothermal systems: Constraints from basalt alteration experiments. *Earth Planet Sci Lett* 101:388–403.
72. Metz S, Trefry JH (2000) Chemical and mineralogical influences on concentrations of trace metals in hydrothermal fluids. *Geochim Cosmochim Acta* 64:2267–2279.
73. Reed MH, Palandri J (2006) Sulfide mineral precipitation from hydrothermal fluids. *Sulfide Mineralogy and Geochemistry*, ed Vaughan DJ (Mineralogical Society of America, Chantilly, VA), pp 609–631.
74. Taran YA, Hedenquist JW, Korzhinsky MA, Tkachenko SI, Shmulovich KI (1995) Geochemistry of magmatic gases from Kudryavy volcano, Iturup, Kuril Islands. *Geochim Cosmochim Acta* 59:1749–1761.
75. Oparin AI (1924) *The Origin of Life* (Moskowskiy Rabochiy, Moscow).
76. Lazcano A, Miller SL (1999) On the origin of metabolic pathways. *J Mol Evol* 49: 424–431.
77. Miller SL, Cleaves HJ (2006) Prebiotic chemistry on the primitive Earth. *Systems Biology: Genomics*, eds Rigoutsos I, Stephanopoulos G (Oxford Univ Press, London), Vol 1, pp 4–56.
78. Sleep NH, Meibom A, Fridriksson T, Coleman RG, Bird DK (2004) H_2-rich fluids from serpentinization: Geochemical and biotic implications. *Proc Natl Acad Sci USA* 101: 12818–12823.
79. Taran YA, Varley NR, Inguaggiato S, Cienfuegos E (2010) Geochemistry of H_2 and CH_4-enriched hydrothermal fluids of Socorro Island, Revillagigedo Archipelago, Mexico. Evidence for serpentinization and abiogenic methane. *Geofluids* 10: 542–555.
80. Brandes JA, et al. (1998) Abiotic nitrogen reduction on the early Earth. *Nature* 395: 365–367.
81. Henglein A (1984) Catalysis of photochemical reactions by colloidal semiconductors. *Pure Appl Chem* 56:1215–1224.
82. Zhang XV, Martin ST, Friend CM, Schoonen MAA, Holland HD (2004) Mineral-assisted pathways in prebiotic synthesis: Photoelectrochemical reduction of carbon (+IV) by manganese sulfide. *J Am Chem Soc* 126:11247–11253.
83. Zhang XV, et al. (2007) Photodriven reduction and oxidation reactions on colloidal semiconductor particles: Implications for prebiotic synthesis. *J Photochem Photobiol Chem* 185:301–311.
84. Guzman MI, Martin ST (2009) Prebiotic metabolism: Production by mineral photoelectrochemistry of alpha-ketocarboxylic acids in the reductive tricarboxylic acid cycle. *Astrobiology* 9:833–842.
85. Liu XF, Ni XY, Wang J, Yu XH (2008) A novel route to photoluminescent, water-soluble Mn-doped ZnS quantum dots via photopolymerization initiated by the quantum dots. *Nanotechnology* 19:485602.
86. Sagan C (1973) Ultraviolet selection pressure on the earliest organisms. *J Theor Biol* 39:195–200.
87. Zhang YC, Wang H, Wang B, Yan H, Yoshimura M (2002) Low-temperature hydrothermal synthesis of pure metastable gamma-manganese sulfide (MnS) crystallites. *J Cryst Growth* 243:214–217.
88. Mitra D, Chakraborty I, Moulik SP (2005) Studies on ZnS nanoparticles prepared in aqueous sodium dodecylsulphate (SDS) micellar medium. *Colloid J* 67:445–450.
89. Biondi E, Branciamore S, Maurel MC, Gallori E (2007) Montmorillonite protection of an UV-irradiated hairpin ribozyme: Evolution of the RNA world in a mineral environment. *BMC Evol Biol* 7(suppl 2):S2.
90. Nold SC, Ward DM (1996) Photosynthate partitioning and fermentation in hot spring microbial mat communities. *Appl Environ Microbiol* 62:4598–4607.
91. Bergaya F, Lagaly G, Vayer M (2006) Cation and anion exchange. *Handbook of Clay Science*, eds Bergaya F, Theng BKG, Lagaly G (Elsevier, Amsterdam), pp 979–1001.
92. Aravind L, Mazumder R, Vasudevan S, Koonin EV (2002) Trends in protein evolution inferred from sequence and structure analysis. *Curr Opin Struct Biol* 12:392–399.
93. Koonin EV, Senkevich TG, Dolja VV (2006) The ancient Virus World and evolution of cells. *Biol Direct* 1:29.
94. Schatz OJ, Dolejs D, Stix J, Williams-Jones AE, Layne GD (2004) Partitioning of boron among melt, brine and vapor in the system haplogranite-H_2O-NaCl at 800° C and 100 MPa. *Chem Geol* 210:135–147.
95. Nikolaeva IY, Bychkov AY (2007) Gas-liquid distribution of boron in hydrotermal springs of Mutnovski volcano. *Herald of the Kamchatka Research Center* 10:34–43.
96. Ricardo A, Carrigan MA, Olcott AN, Benner SA (2004) Borate minerals stabilize ribose. *Science* 303:196.
97. Grew ES, Bada JL, Hazen RM (2011) Borate minerals and origin of the RNA world. *Orig Life Evol Biosph* 41:307–316.
98. Harada K (1967) Formation of amino-acids by thermal decomposition of formamide - oligomerization of hydrogen cyanide. *Nature* 214:479.
99. Schoffstall AM, Laing EM (1984) Equilibration of nucleotide derivatives in formamide. *Orig Life Evol Biosph* 14:221–228.
100. Schoffstall AM (1976) Prebiotic phosphorylation of nucleosides in formamide. *Orig Life* 7:399–412.
101. Schoffstall AM, Barto RJ, Ramos DL (1982) Nucleoside and deoxynucleoside phosphorylation in formamide solutions. *Orig Life* 12:143–151.
102. Schoffstall AM, Mahone SM (1988) Formate ester formation in amide solutions. *Orig Life Evol Biosph* 18:389–396.
103. Saladino R, Crestini C, Costanzo G, Negri R, Di Mauro E (2001) A possible prebiotic synthesis of purine, adenine, cytosine, and 4(3H)-pyrimidinone from formamide: Implications for the origin of life. *Bioorg Med Chem* 9:1249–1253.
104. Saladino R, Crestini C, Ciciriello F, Costanzo G, Di Mauro E (2006) About a formamide-based origin of informational polymers: Syntheses of nucleobases and favourable thermodynamic niches for early polymers. *Orig Life Evol Biosph* 36: 523–531.
105. Costanzo G, Saladino R, Crestini C, Ciciriello F, Di Mauro E (2007) Formamide as the main building block in the origin of nucleic acids. *BMC Evol Biol* 7(suppl 2):S1.
106. Costanzo G, Saladino R, Crestini C, Ciciriello F, Di Mauro E (2007) Nucleoside phosphorylation by phosphate minerals. *J Biol Chem* 282:16729–16735.
107. Saladino R, Crestini C, Ciciriello F, Costanzo G, Di Mauro E (2007) Formamide chemistry and the origin of informational polymers. *Chem Biodivers* 4:694–720.
108. Saladino R, et al. (2009) From formamide to RNA: The roles of formamide and water in the evolution of chemical information. *Res Microbiol* 160:441–448.
109. Mukhin LM (1976) Volcanic processes and synthesis of simple organic compounds on primitive earth. *Orig Life* 7:355–368.
110. Holloway JM, Dahlgren RA (2002) Nitrogen in rock: Occurrences and biogeochemical implications. *Global Biogeochem Cycles* 16:1118.
111. Saladino R, et al. (2004) Synthesis and degradation of nucleobases and nucleic acids by formamide in the presence of montmorillonites. *ChemBioChem* 5:1558–1566.
112. Saladino R, et al. (2003) One-pot TiO_2-catalyzed synthesis of nucleic bases and acyclonucleosides from formamide: implications for the origin of life. *ChemBioChem* 4:514–521.
113. Shanker U, Bhushan B, Bhattacharjee G, Kamaluddin (2011) Formation of nucleobases from formamide in the presence of iron oxides: Implication in chemical evolution and origin of life. *Astrobiology* 11:225–233.
114. Saladino R, et al. (2005) Origin of informational polymers. Differential stability of 3′- and 5′-phosphoester bonds in deoxy monomers and oligomers. *J Biol Chem* 280: 35658–35669.
115. Saladino R, Crestini C, Ciciriello F, Di Mauro E, Costanzo G (2006) Origin of informational polymers: differential stability of phosphoester bonds in ribomonomers and ribooligomers. *J Biol Chem* 281:5790–5796.
116. Bernal JD (1951) *The Physical Basis of Life* (Routledge and Kegan Paul, London).
117. Nisbet EG (1986) RNA and hot-water springs. *Nature* 322:206.
118. Ferris JP (2006) Montmorillonite-catalysed formation of RNA oligomers: The possible role of catalysis in the origins of life. *Philos Trans R Soc Lond B Biol Sci* 361: 1777–1786.
119. Sobolewski AL, Domcke W (2006) The chemical physics of the photostability of life. *Europhys News* 37:20–23.
120. Senanayake SD, Idriss H (2006) Photocatalysis and the origin of life: Synthesis of nucleoside bases from formamide on TiO_2(001) single surfaces. *Proc Natl Acad Sci USA* 103:1194–1198.
121. Powner MW, Gerland B, Sutherland JD (2009) Synthesis of activated pyrimidine ribonucleotides in prebiotically plausible conditions. *Nature* 459:239–242.
122. Barks HL, et al. (2010) Guanine, adenine, and hypoxanthine production in UV-irradiated formamide solutions: Relaxation of the requirements for prebiotic purine nucleobase formation. *ChemBioChem* 11:1240–1243.
123. Gilbert W (1986) The RNA world. *Nature* 319:618.
124. Serrano-Andres L, Merchan M (2009) Are the five natural DNA/RNA base monomers a good choice from natural selection? A photochemical perspective. *J Photochem Photobiol Photochem Rev* 10:21–32.
125. van Roode JHG, Orgel LE (1980) Template-directed synthesis of oligoguanylates in the presence of metal ions. *J Mol Biol* 144:579–585.
126. Haldane JBS (1929) The Origin of Life. *The Rationalist Annual*, ed Watts CA (Watts, London), pp 3–10.
127. Russell MJ, Hall AJ, Cairns-Smith AG, Braterman PS (1988) Submarine hot springs and the origin of life. *Nature* 336:117.

128. Martin W, Russell MJ (2003) On the origins of cells: A hypothesis for the evolutionary transitions from abiotic geochemistry to chemoautotrophic prokaryotes, and from prokaryotes to nucleated cells. *Philos Trans R Soc Lond B Biol Sci* 358:59–83.
129. Martin W, Baross J, Kelley D, Russell MJ (2008) Hydrothermal vents and the origin of life. *Nat Rev Microbiol* 6:805–814.
130. Kim KM, Caetano-Anollés G (2011) The proteomic complexity and rise of the primordial ancestor of diversified life. *BMC Evol Biol* 11:140.
131. Mulkidjanian AY, Dibrov P, Galperin MY (2008) The past and present of sodium energetics: May the sodium-motive force be with you. *Biochim Biophys Acta* 1777:985–992.
132. Mulkidjanian AY, Galperin MY, Makarova KS, Wolf YI, Koonin EV (2008) Evolutionary primacy of sodium bioenergetics. *Biol Direct* 3:13.
133. Ponnamperuma C, Mariner R, Sagan C (1963) Formation of adenosine by ultra-violet irradiation of a solution of adenine and ribose. *Nature* 198:1199–1200.
134. Hanczyc MM, Fujikawa SM, Szostak JW (2003) Experimental models of primitive cellular compartments: encapsulation, growth, and division. *Science* 302:618–622.
135. Monnard PA, Szostak JW (2008) Metal-ion catalyzed polymerization in the eutectic phase in water-ice: A possible approach to template-directed RNA polymerization. *J Inorg Biochem* 102:1104–1111.
136. Saladino R, et al. (2011) Photochemical synthesis of citric acid cycle intermediates based on titanium dioxide. *Astrobiology* 11:815–824.
137. Kritsky MS, Kolesnikov MP, Telegina TA (2007) Modeling of abiogenic synthesis of ATP. *Dokl Biochem Biophys* 417:313–315.
138. Clynne MA, Janik CJ, Muffer LJP (2003) *"Hot Water" in Lassen Volcanic National Park— Fumaroles, Steaming Ground, and Boiling Mudpots* (US Geological Survey, Menlo Park, CA).
139. Gunnarsson B, Marsh BD, Taylor HP (1998) Generation of Icelandic rhyolites: Silicic lavas from the Torfajokull central volcano. *J Volcanol Geotherm Res* 83:1–45.
140. Ushikubo T, et al. (2008) Lithium in Jack Hills zircons: Evidence for extensive weathering of Earth's earliest crust. *Earth Planet Sci Lett* 272:666–676.
141. Walker JCG (1985) Carbon dioxide on the early earth. *Orig Life Evol Biosph* 16: 117–127.
142. Williams RJP, Frausto da Silva JJR (1991) *The Biological Chemistry of the Elements* (Clarendon, Oxford).
143. Zhang YS, Zhang ZY, Suzuki K, Maekawa T (2003) Uptake and mass balance of trace metals for methane producing bacteria. *Biomass Bioenergy* 25:427–433.
144. Nies DH (2007) Bacterial transition metal homeostasis. *Molecular Microbiology of Heavy Metals*, eds Nies DH, Silver S (Springer-Verlag, Berlin), pp 117–142.
145. Nies DH, Silver S, eds (2007) *Molecular Microbiology of Heavy Metals* (Springer-Verlag, Berlin).

Supporting Information to the paper by A.Y. Mulkidjanian et al.
"Origin of first cells at terrestrial, anoxic geothermal fields".

Table S1. Products of ubiquitous genes and their association with essential inorganic cations and anions.

The lists of ubiquitous genes were extracted from refs. (1, 2). The data on the dependence of functional activity on particular metals were taken from the BRENDA database (3). According to the BRENDA database, the enzymatic activity of most Mg^{2+}-dependent enzymes could be routinely restored by Mn^{2+}. As concentration of Mg^{2+} ions in the cell is ca. 10^{-2} M, whereas that of Mn^{2+} ions is ca. 10^{-6} M, the data on the functional importance of Mn^{2+} were not included in the table for many enzymes. The presence of metals in protein structures was as listed in the Protein Data Bank (4) entries. The table includes all enzymes represented by orthologs in all cellular life forms as well as several cases when a function is ubiquitous (e.g., DNA polymerase, DNA primase) whereas the enzymes responsible for that function are represented by two or more non-orthologous forms (5). Upward arrows indicate the activation by the particular ion and downward arrows indicate the inhibition by this ion. If low ion concentrations activate the enzyme while high amounts of the same ion cause its inhibition then the ↑↓ sign is used.

Protein function	EC number (if available)	Functionally relevant inorganic anions	Functional dependence on monovalent cations	Monovalent cations in at least some structures	Functional dependence on divalent cations	Divalent cations in at least some structures
Products of ubiquitous genes, according to (Koonin 2000 (1))						
Ribosome as whole	-	-	K^+ (6, 7)	K^+, Na^+ (in the 1JJ2 structure) *	Mg^{2+} (8)	Mg^{2+} (1JJ2, 3OH7, 1MMS), Cd^{2+}(1MMS) †, Zn^{2+} (1HR0)
Ribosomal protein L1	-	-	-	-	-	-
Ribosomal protein L10	-	-	-	-	-	-
Ribosomal protein L11	-	-	-	-	-	Mg^{2+}, Cd^{2+} (1MMS)
Ribosomal protein L13	-	-	-	K^+, Na^+ (1JJ2)	-	-
Ribosomal protein L14	-	-	-	-	-	-
Ribosomal protein L15	-	-	-	K^+, Na^+ (1JJ2)	-	Mg^{2+} (3OH7)
Ribosomal protein L16/L10E	-	-	-	K^+, Na^+ (1JJ2)	-	Mg^{2+} (3OH7)
Ribosomal protein L18	-	-	-	-	-	-
Ribosomal protein L2	-	-	-	K^+, Na^+ (1JJ2)	-	Mg^{2+} (1JJ2, 3OH7)
Ribosomal protein L22	-	-	-	K^+, Na^+ (1JJ2)	-	
Ribosomal protein L24	-	-	-	K^+, Na^+ (1JJ2)	-	Mg^{2+} (1JJ2)
Ribosomal protein L29	-	-	-	-	-	-
Ribosomal protein L3	-	-	-	K^+, Na^+ (1JJ2)	-	Mg^{2+} (1JJ2, 3OH7)
Ribosomal protein L4	-	-	-	K^+, Na^+ (1JJ2)	-	Mg^{2+} (3OH7)
Ribosomal protein L5	-	-	-	-	-	-
Ribosomal protein L6	-	-	-	-	-	-

* Upon the crystallization of the ribosomes of *H. marismortui*, the media contained 1.7 M of Na^+, so that mostly Na^+ ions are observed in the 1JJ2 structure. *H. marismortui* is a halophylic archaea and can accumulate up to 3M K^+ under high salt conditions; thus the Na^+-containing sites in the 1JJ2 structure should be mostly occupied by K^+ ions *in vivo*, as in other ribosomal structures.

†† Here and below Cd^{2+} is not a native cofactor. High amounts of $CdCl_2$ were added upon ribosome crystallization to improve the phasing. Other divalent cations occupy the place of Cd^{2+} ions in the native ribosome, see a detailed discussion in (9).

Ribosomal protein S10	-	-	-	-	-	-
Ribosomal protein S11	-	-	-	-	-	-
Ribosomal protein S12	-	-	-	-	-	Mg^{2+} (3OH7)
Ribosomal protein S13	-	-	-	-	-	-
Ribosomal protein S14	-	-	-	-	-	Zn^{2+} (1HR0)
Ribosomal protein S15	-	-	-	-	-	-
Ribosomal protein S17	-	-	-	-	-	-
Ribosomal protein S19	-	-	-	-	-	-
Ribosomal protein S2	-	-	-	-	-	-
Ribosomal protein S3	3.1.25.1	-	-	-	-	-
Ribosomal protein S5	-	-	-	-	-	-
Ribosomal protein S7	-	-	-	-	-	-
Ribosomal protein S8	-	-	-	-	-	-
Ribosomal protein S9	-	-	-	-	-	-
Translation elongation factor G (EF-2)	3.6.5.3	phosphate	$\uparrow NH_4^+$, $\downarrow Na^+$ (10)	-	Mg^{2+}	Mg^{2+} (1WRI)
Translation elongation factor Tu (EF-1)	3.6.5.3	phosphate	$\uparrow NH_4^+$, K^+, $\downarrow Na^+$ (10, 11)	-	Mg^{2+}/Mn^{2+}	Mg^{2+} (2XQD)
Translation initiation factor 2	3.6.5.3	$phosphate^-$	$\uparrow NH_4^+$, $\downarrow Na^+$ (10)	-	Mg^{2+}, Zn^{2+} (β subunit) (12)	Mg^{2+} (1G7T), Zn^{2+} (2QMU, 2D74)
Translation initiation factor IF-1	3.6.5.3	phosphate	$\uparrow NH_4^+$, $\downarrow Na^+$ (10)	-	Mg^{2+}	Mg^{2+} (1HR0)
Translation elongation factor P/ translation initiatiation factor eIF5-a	-	-	-	-	-	No metals seen
Seryl-tRNA synthetase	6.1.1.11	pyrophosphate	$\downarrow K^+$ (13)	Na^+	Mg^{2+} (14), Zn^{2+} (15)	Mg^{2+}, Zn^{2+}
Methionyl-tRNA synthetase	6.1.1.10	pyrophosphate	-	-	Mg^{2+} (16), Zn^{2+} (17)	Zn^{2+}
Histidyl-tRNA synthetase	6.1.1.21	pyrophosphate	-	-	Mg^{2+} (18)	-
Tryptophanyl-tRNA synthetase	6.1.1.2	pyrophosphate	$\downarrow K^+$ (13)	Cs^+	Mg^{2+}, Zn^{2+} (19)	Mg^{2+}, Ca^{2+}, ‡Cd^{2+}
Tyrosyl-tRNA synthetase	6.1.1.1	pyrophosphate	$\uparrow K^+$, $\downarrow Na^+$ (20), $\uparrow K^+$ (21)	K^+	Mg^{2+} (20, 22, 23)	Mg^{2+}
Phenylalanyl-tRNA synthetase	6.1.1.20	pyrophosphate	-	-	Mg^{2+} (18), Zn^{2+} (24, 25)	Mg^{2+}/Mn^{2+}, Zn^{2+}
Aspartyl-tRNA synthetase	6.1.1.12	pyrophosphate	$\uparrow\downarrow K^+$, $\downarrow Na^+$ (26)	-	Mg^{2+} (27)	Mg^{2+}/Mn^{2+}
Valyl-tRNA synthetase	6.1.1.9	pyrophosphate	$\uparrow\downarrow K^+$ (13)	-	Mg^{2+} (28)	Zn^{2+}
Isoleucyl-tRNA synthetase	6.1.1.5	pyrophosphate	-	K^+	Mg^{2+} (18), Zn^{2+} (29)	Mg^{2+}, Zn^{2+}
Leucyl-tRNA synthetase	6.1.1.4	pyrophosphate	-	-	Mg^{2+} (30)	Zn^{2+}, Hg^{2+}
Threonyl-tRNA synthetase	6.1.1.3	pyrophosphate	-	-	Mg^{2+} (31), Zn^{2+} (32)	Zn^{2+}
Arginyl-tRNA synthetase	6.1.1.19	pyrophosphate	$\downarrow K^+$ (33)	-	Mg^{2+} (18)	Mg^{2+}
Prolyl-tRNA synthetase	6.1.1.15	pyrophosphate	-	-	Mg^{2+} (34), Zn^{2+} (35)	Mg^{2+}/Mn^{2+}, Zn^{2+}
Alanyl-tRNA synthetase	6.1.1.7	pyrophosphate	-	-	Mg^{2+}, Zn^{2+} (36)	Mg^{2+}, Zn^{2+}
Pseudouridylate synthase	5.4.99.12	-	K^+ (37)	K^+	Zn^{2+} (38)	Zn^{2+}
Methionine aminopeptidase	3.4.11.18	-	-	$K^+ > Na^+$	Zn^{2+}, Mn^{2+}, Co^{2+}, Ni^{2+}, Fe^{2+} (35, 39, 40)	Mn^{2+}/Zn^{2+}/ $Co^{2+}/Ni^{2+}/Fe^{2+}$
Transcription antiterminator NusG	-	-	-	-	-	No metals seen
DNA-directed RNA polymerase, subunits α, β, β'	2.7.7.6	pyrophosphate	-	Na^+ (3K4G)	Mg^{2+} (41), Zn^{2+} (42)	Mg^{2+}/Mn^{2+}, Zn^{2+}
DNA polymerase III, subunit β (sliding clamp)	2.7.7.7	-	-	-	-	
Clamp loader ATPase (DNA polymerase III, subunit γ and τ)	2.7.7.7	phosphate	-	-	Mg^{2+}	Mg^{2+}, Zn^{2+}
Topoisomerase IA	5.99.1.2	-	$K^+ > Na^+$ (43)	-	Mg^{2+} (44)	Zn^{2+} (1CCY)
5'-3' exonuclease (including N-terminal domain of PolI)	3.1.11.[a]	phosphate	-	-	Mg^{2+} (45)	Mn^{2+} (1UT5),

‡ Cd^{2+} do not occur in native protein structures but could be used to improve phasing during structure obtaining. It occupies the binding sites of other divalent metals.

	a = 3-6 (5→3) a = 1-2 (3->5)					Zn^{2+} (1TAQ)
RecA/RadA (Rad51) recombinase	-	phosphate	K^+ (46)	K^+ (1XU4)	Mg^{2+} (47)	Mg^{2+} (1T4G)
Chaperonin GroEL	3.6.4.9	phosphate	K^+ (48)	K^+	Mg^{2+} (49)	Mg^{2+}
O-sialoglycoprotease (MG2+046, PF00814) (50)/ apurinic endonuclease (51)	3.4.24.57	phosphate	-	-	Zn^{2+} (52), Fe^{2+} (51)	Mg^{2+} (1IVN, 3ENO)
EMAP domain (OB-fold RNA-binding domain, MG2+449, PF01588)	-	-	-	-	-	-
Thymidylate kinase	2.7.4.9	phosphate	-	Na^+ (2WWF)	Mg^{2+} (53)	Mg^{2+}
Thioredoxin reductase	1.8.1.9	-	-	-	-	Mg^{2+} (2A87)
Thioredoxin	-	-	-	-	-	Cd^{2+} (3KD0) [§], Zn^{2+} (3P2A, 2XC2, 3HXS)
CDP-diglyceride-synthase	2.7.7.41	pyrophosphate	↑K^+, NH_4^+, Rb^+ ↓Li^+, Na^+ Cs^+ (54)	No entries	Mg^{2+} (54)	No entries
Phosphomannomutase	5.4.2.8	-	-	-	Mg^{2+} (55)	Mg^{2+}/Zn^{2+}
Catalytic subunit of the membrane ATP synthase	3.6.3.14	phosphate	-	-	Mg^{2+} (56, 57)	Mg^{2+}
Proteolipid subunits of the membrane ATP synthase	3.6.3.14	-	-	-	-	No metals seen
Triosephosphate isomerase	5.3.1.1	-	-	-	-	No metals seen
Glycine hydroxymethyltransferase	2.1.2.1	-	↓K^+, NH_4^+, Na^+ (58, 59)	-	↓Mg^{2+}, Mn^{2+}, Ca^{2+} (58, 59)	No metals seen
Preprotein translocase subunit SecY	-	-	-	-	-	Zn^{2+} (2ZJS)
Signal recognition particle GTPase FtsY	3.6.5.4	$phosphate^-$	-	K^+ (2J7P)	Mg^{2+} (60)	Mg^{2+}
Predicted GTPase (YchF, PF06071, 1JAL, 2OHF, 2DBY, 2DWQ, 1NI3)	-	phosphate	K^+ (61)	-	Mg^{2+} (62)	No metals seen
Additional ubiquitous gene products from ref. (Charlebois and Doolittle 2004 (2))						
DNA primase (dnaG)	2.7.7.-	pyrophosphate	-	-	Zn^{2+} (63)	Zn^{2+} (2AU3, 1D0Q)
S-adenosylmethionine-6-N',N'-adenosyl (rRNA) dimethyltransferase (KsgA)	2.1.1.48	-	-	-	Mg^{2+} (64)	No metals seen
Transcription pausing, L factor (NusA)	-	-	-	-	-	No metals seen

References

1. Koonin EV (2000) How many genes can make a cell: the minimal-gene-set concept. *Annu. Rev. Genom. Human Genet* 1:99-116.
2. Charlebois RL & Doolittle WF (2004) Computing prokaryotic gene ubiquity: rescuing the core from extinction. *Genome Res* 14:2469-2477.
3. Chang A, Scheer M, Grote A, Schomburg I, & Schomburg D (2009) BRENDA, AMENDA and FRENDA the enzyme information system: new content and tools in 2009. *NAR* 37:D588-592.
4. Berman HM*, et al.* (2000) The Protein Data Bank. *Nucl Acids Res* 28:235-242.
5. Koonin EV (2003) Comparative genomics, minimal gene-sets and the last universal common ancestor. *Nat Rev Microbiol* 1:127-136.
6. Michelinaki M, Spanos A, Coutsogeorgopoulos C, & Kalpaxis DL (1997) New aspects on the kinetics of activation of ribosomal peptidyltransferase-catalyzed peptide bond formation by monovalent ions and spermine. *Biochim Biophys Acta* 1342:182-190.
7. Ioannou M & Coutsogeorgopoulos C (1997) Kinetic studies on the activation of eukaryotic peptidyltransferase by potassium. *Arch Biochem Biophys* 345:325-331.

[§] Cd^{2+} do not occur in native protein structures. This PDB file refers to a structure of special fourfold Cys→Ser mutant which was obtained in the presence of Cd salts.

8. Hsiao C & Williams LD (2009) A recurrent magnesium-binding motif provides a framework for the ribosomal peptidyl transferase center. *Nucleic Acids Res* 37:3134-3142.
9. Mulkidjanian AY & Galperin MY (2009) On the origin of life in the zinc world. 2. Validation of the hypothesis on the photosynthesizing zinc sulfide edifices as cradles of life on Earth. *Biol Direct* 4:27.
10. Conway TW (1964) On the role of ammonium or potassium ion in amino acid polymerization. *Proc. Natl. Acad. Sci. USA* 51:1216-1220.
11. Fasano O, De Vendittis E, & Parmeggiani A (1982) Hydrolysis of GTP by elongation factor Tu can be induced by monovalent cations in the absence of other effectors. *J Biol Chem* 257:3145-3150.
12. Donahue TF, Cigan AM, Pabich EK, & Valavicius BC (1988) Mutations at a Zn(II) finger motif in the yeast eIF-2 beta gene alter ribosomal start-site selection during the scanning process. *Cell* 54:621-632.
13. Jukubowski H & Pawelkiewicz J (1975) The plant aminoacyl-tRNA synthetases. Purification and characterization of valyl-tRNA, tryptophanyl-tRNA and seryl-tRNA synthetases from yellow-lupin seeds. *Eur J Biochem* 52:301-310.
14. Pachmann U & Zachau HG (1978) Yeast seryl tRNA synthetase: two sets of substrate sites involved in aminoacylation. *Nucleic Acids Res* 5:961-973.
15. Bilokapic S*, et al.* (2006) Structure of the unusual seryl-tRNA synthetase reveals a distinct zinc-dependent mode of substrate recognition. *EMBO J* 25:2498-2509.
16. Deobagkar DN & Gopinathan KP (1976) Two forms of methionyl-transfer RNA synthetase from *Mycobacterium smegmatis*. *Biochem Biophys Res Commun* 71:939-951.
17. Fourmy D, Mechulam Y, & Blanquet S (1995) Crucial role of an idiosyncratic insertion in the Rossman fold of class 1 aminoacyl-tRNA synthetases: the case of methionyl-tRNA synthetase. *Biochemistry* 34:15681-15688.
18. Airas RK (1996) Differences in the magnesium dependences of the class I and class II aminoacyl-tRNA synthetases from *Escherichia coli*. *Eur J Biochem* 240:223-231.
19. Kisselev LL (1993) Mammalian tryptophanyl-tRNA synthetases. *Biochimie* 75:1027-1039.
20. Austin J & First EA (2002) Catalysis of tyrosyl-adenylate formation by the human tyrosyl-tRNA synthetase. *J Biol Chem* 277:14812-14820.
21. Warner CK & Jacobson KB (1976) Mechanisms of suppression in *Drosophila*. IV. Specificity and properties of tyrosyl-tRNA synthetase. *Can J Biochem* 54:650-656.
22. Brown P*, et al.* (1999) Molecular recognition of tyrosinyl adenylate analogues by prokaryotic tyrosyl tRNA synthetases. *Bioorg Med Chem* 7:2473-2485.
23. Hamano-Takaku F*, et al.* (2000) A mutant *Escherichia coli* tyrosyl-tRNA synthetase utilizes the unnatural amino acid azatyrosine more efficiently than tyrosine. *J Biol Chem* 275:40324-40328.
24. Brevet A, Plateau P, Cirakoglu B, Pailliez JP, & Blanquet S (1982) Zinc-dependent synthesis of 5',5'-diadenosine tetraphosphate by sheep liver lysyl- and phenylalanyl-tRNA synthetases. *J Biol Chem* 257:14613-14615.
25. Plateau P, Mayaux JF, & Blanquet S (1981) Zinc(II)-dependent synthesis of diadenosine 5', 5''' -P(1) ,P(4) -tetraphosphate by Escherichia coli and yeast phenylalanyl transfer ribonucleic acid synthetases. *Biochemistry* 20:4654-4662.
26. Vellekamp GJ & Kull FJ (1981) Allotropism in aspartyl-tRNA synthetase from procine thyroid. *Eur J Biochem* 118:261-269.
27. Norton SJ, Ravel JM, Lee C, & Shive W (1963) Purification and properties of the aspartyl ribonucleic acid synthetase of *Lactobacillus arabinosus*. *J Biol Chem* 238:269-274.
28. Godar DE & Yang DC (1988) Mammalian high molecular weight and monomeric forms of valyl-tRNA synthetase. *Biochemistry* 27:2181-2186.
29. Glasfeld E, Landro JA, & Schimmel P (1996) C-terminal zinc-containing peptide required for RNA recognition by a class I tRNA synthetase. *Biochemistry* 35:4139-4145.
30. Chirikjian JG, Kanagalingam K, Lau E, & Fresco JR (1973) Purification and properties of leucyl-tRNA synthetase from Bakers' yeast. *J Biol Chem* 248:1074-1079.
31. Freist W & Gauss DH (1995) Threonyl-tRNA synthetase. *Biol Chem Hoppe Seyler* 376:213-224.

32. Sankaranarayanan R*, et al.* (1999) The structure of threonyl-tRNA synthetase-tRNA(Thr) complex enlightens its repressor activity and reveals an essential zinc ion in the active site. *Cell* 97:371-381.
33. Airas RK (2006) Analysis of the kinetic mechanism of arginyl-tRNA synthetase. *Biochim Biophys Acta* 1764:307-319.
34. Peterson PJ & Fowden L (1965) Purification, properties and comparative specificities of the enzyme prolyl-transfer ribonucleic acid synthetase from *Phaseolus aureus* and Polygonatum multiflorum. *Biochem J* 97:112-124.
35. Kamtekar S*, et al.* (2003) The structural basis of cysteine aminoacylation of tRNAPro by prolyl-tRNA synthetases. *Proc Natl Acad Sci USA* 100:1673-1678.
36. Sood SM, Wu MX, Hill KA, & Slattery CW (1999) Characterization of zinc-depleted alanyl-tRNA synthetase from *Escherichia coli*: role of zinc. *Arch Biochem Biophys* 368:380-384.
37. Green CJ, Kammen HO, & Penhoet EE (1982) Purification and properties of a mammalian tRNA pseudouridine synthase. *J Biol Chem* 257:3045-3052.
38. Arluison V, Hountondji C, Robert B, & Grosjean H (1998) Transfer RNA-pseudouridine synthetase Pus1 of *Saccharomyces cerevisiae* contains one atom of zinc essential for its native conformation and tRNA recognition. *Biochemistry* 37:7268-7276.
39. Ben-Bassat A*, et al.* (1987) Processing of the initiation methionine from proteins: properties of the *Escherichia coli* methionine aminopeptidase and its gene structure. *J Bacteriol* 169:751-757.
40. Wang WL*, et al.* (2008) Discovery of inhibitors of *Escherichia coli* methionine aminopeptidase with the Fe(II)-form selectivity and antibacterial activity. *J Med Chem* 51:6110-6120.
41. Sosunov V*, et al.* (2003) Unified two-metal mechanism of RNA synthesis and degradation by RNA polymerase. *EMBO J* 22:2234-2244.
42. King RA, Markov D, Sen R, Severinov K, & Weisberg RA (2004) A conserved zinc binding domain in the largest subunit of DNA-dependent RNA polymerase modulates intrinsic transcription termination and antitermination but does not stabilize the elongation complex. *J Mol Biol* 342:1143-1154.
43. Ivanov VA, Melnikov AA, & Terpilovska ON (1986) DNA topoisomerase I from rat brain neurons. *Biochim Biophys Acta* 866:154-160.
44. Sutcliffe JA, Gootz TD, & Barrett JF (1989) Biochemical characteristics and physiological significance of major DNA topoisomerases. *Antimicrob Agents Chemother* 33:2027-2033.
45. Dolberg M, Baur CP, & Knippers R (1991) Purification and characterization of a novel 5' exodeoxyribonuclease from the yeast *Saccharomyces cerevisiae*. *Eur J Biochem* 198:783-787.
46. Wu Y, Qian X, He Y, Moya IA, & Luo Y (2005) Crystal structure of an ATPase-active form of Rad51 homolog from *Methanococcus voltae*. Insights into potassium dependence. *J Biol Chem* 280:722-728.
47. Muller B, Burdett I, & West SC (1992) Unusual stability of recombination intermediates made by Escherichia coli RecA protein. *EMBO J* 11:2685-2693.
48. Viitanen PV*, et al.* (1990) Chaperonin-facilitated refolding of ribulosebisphosphate carboxylase and ATP hydrolysis by chaperonin 60 (groEL) are K^+ dependent. *Biochemistry* 29:5665-5671.
49. Horovitz A, Fridmann Y, Kafri G, & Yifrach O (2001) Review: allostery in chaperonins. *J Struct Biol* 135:104-114.
50. Katz C, Cohen-Or I, Gophna U, & Ron EZ (2010) The ubiquitous conserved glycopeptidase gcp prevents accumulation of toxic glycated proteins. *MBio* 1:3e00195-10.
51. Hecker A*, et al.* (2007) An archaeal orthologue of the universal protein Kae1 is an iron metalloprotein which exhibits atypical DNA-binding properties and apurinic-endonuclease activity in vitro. *Nucleic Acids Res* 35:6042-6051.
52. Abdullah KM, Lo RY, & Mellors A (1991) Cloning, nucleotide sequence, and expression of the *Pasteurella haemolytica* A1 glycoprotease gene. *J Bacteriol* 173:5597-5603.
53. Nelson DJ & Carter CE (1969) Purification and characterization of Thymidine 5-monophosphate kinase from *Escherichia coli B*. *J Biol Chem* 244:5254-5262.
54. McCaman RE & Finnerty WR (1968) Biosynthesis of cytidine diphosphate-diglyceride by a particulate fracgion from *Micrococcus cerificans*. *J Biol Chem* 243:5074-5080.

55. Guha SK & Rose ZB (1985) The synthesis of mannose 1-phosphate in brain. *Arch Biochem Biophys* 243:168-173.

56. Satoh S, Moritani C, Ohhashi T, Konishi K, & Ikeda M (1994) Chloroplast ATPase in *Acetabularia acetabulum*: purification and characterization of chloroplast F1-ATPase. *Biosci Biotechnol Biochem* 58:521-525.

57. Ferguson SA, Keis S, & Cook GM (2006) Biochemical and molecular characterization of a Na+-translocating F1Fo-ATPase from the thermoalkaliphilic bacterium *Clostridium paradoxum*. *J Bacteriol* 188:5045-5054.

58. Fujioka M (1969) Purification and properties of serine hydroxymethylase from soluble and mitochondrial fractions of rabbit liver. *Biochim Biophys Acta* 185:338-349.

59. Nakamura KD, Trewyn RW, & Parks LW (1973) Purification and characterization of serine transhydroxy-methylase from Saccharomyces cerevisiae. *Biochim Biophys Acta* 327:328-335.

60. Bange G, Wild K, & Sinning I (2007) Protein translocation: checkpoint role for SRP GTPase activation. *Curr Biol* 17:R980-982.

61. Anand B, Surana P, & Prakash B (2010) Deciphering the catalytic machinery in 30S ribosome assembly GTPase YqeH. *PLoS One* 5:e9944.

62. Teplyakov A*, et al.* (2003) Crystal structure of the YchF protein reveals binding sites for GTP and nucleic acid. *J Bacteriol* 185:4031-4037.

63. Pan H & Wigley DB (2000) Structure of the zinc-binding domain of *Bacillus stearothermophilus* DNA primase. *Structure* 8:231-239.

64. Andresson OS & Davies JE (1980) Some properties of the ribosomal RNA methyltransferase encoded by ksgA and the polarity of ksgA transcription. *Mol Gen Genet* 179:217-222.

The K^+ binding motif in the P-loop GTPases

In the Ras GTPase, the best studied of the P-loop GTPases, the hydrolysis of GTP is controlled by the interaction between the GTPase and the GTPase Activating Protein (GAP). The transition state is stabilized by the catalytic Gln (Gln^{cat}) residue of Ras while insertion of the Arg^{GAP} residue of GAP (the so-called "arginine finger") stimulates the hydrolysis. This mechanism, however, does not apply to a large number of different GTPases which lack the Gln^{cat} residue and do not require additional protein (i.e. GAP) for the effective hydrolysis of GTP (1). These proteins were named HAS-GTPases after the Hydrophobic Amino Acid Substitution which takes place in the Gln^{cat} position.

For a number of proteins referred to as HAS-GTPases, the hydrolysis of GTP was found to be potassium-dependent but not sodium-dependent (**Table S2**). For some of these enzymes, the K^+-binding motifs have been identified; it has been suggested that, upon activation, the K^+ ion plays the same role as the "arginine finger" in Ras (2-4).

As early as in 1964, Conwey and Lipmann have shown that the protein synthesis and the GTP hydrolysis by ribosomes were concurrently stimulated by K^+ and NH_4^+, but suppressed by Na^+ and Li^+ (6, 7). We checked if known translation factors (which fall into the same TRAFAC superfamily of GTPases as the potassium-dependent proteins from **Table S2**) possess the respective sequence motif for K^+ binding (2).

Translation factors from organisms representing the three domains of life were aligned with K^+-dependent GTPases listed in **Table S2**. Functionally important and conserved parts of the alignment are presented on **Figure S2**. Critically important Asn residue in the P-loop (marked with bold red arrow) is changed into Asp in all translation factors but this particular change was found not to affect the K^+-dependence of the GTPase activity of the YqeH GTPase in a notable way (2).

The second important residue, Gly in the Switch I, is conserved in most translation factors. Both residues are not well-conserved in the overall TRAFAC superfamily of the GTPases (see **Figure S4**), in contrast with the key residues of the conserved nucleotide-binding motifs.

We propose that translation factors could be activated by potassium in the same way as the studied K^+-dependent GTPases do. Although no potassium ion was detected so far in the crystal structures of the

translation factors, orientation of the tentative K^+ ligands seems to be very similar to the one observed in the MnmE structure (**Figure S3**).

Notably, not only the translation factor GTPases but also some of the ubiquitous ATPases are K^+-dependent (Tables 2 and S1).

References

1. Mishra R, Gara SK, Mishra S, & Prakash B (2005) Analysis of GTPases carrying hydrophobic amino acid substitutions in lieu of the catalytic glutamine: implications for GTP hydrolysis. *Proteins* 59:332-338.
2. Anand B, Surana P, & Prakash B (2010) Deciphering the catalytic machinery in 30S ribosome assembly GTPase YqeH. *PLoS One* 5:e9944.
3. Scrima A & Wittinghofer A (2006) Dimerisation-dependent GTPase reaction of MnmE: how potassium acts as GTPase-activating element. *EMBO J* 25:2940-2951.
4. Ash MR*, et al.* (2010) Potassium-activated GTPase reaction in the G Protein-coupled ferrous iron transporter B. *J Biol Chem* 285:14594-14602.
5. Yamanaka K, Hwang J, & Inouye M (2000) Characterization of GTPase activity of TrmE, a member of a novel GTPase superfamily, from *Thermotoga maritima*. *J Bacteriol* 182:7078-7082.
6. Conway TW & Lipmann F (1964) Characterization of a ribosome-linked guanosine triphosphatase in *Escherichia coli* extracts. *Proc Natl Acad Sci USA* 52:1462-1469.
7. Conway TW (1964) On the Role of Ammonium or Potassium Ion in Amino Acid Polymerization. *Proc Natl Acad Sci USA* 51:1216-1220.
8. Leipe DD, Wolf YI, Koonin EV, & Aravind L (2002) Classification and evolution of P-loop GTPases and related ATPases. *J Mol Biol* 317:41-72.

Table S2. Potassium-dependent GTPases. For MnmE, the K atom is seen in the structure (PDB ID 2GJ8, **Figure S1**)

#	*Gene name*	*Protein ID*	*Organism*	*Effects of K^+ and Na^+, reference*
1	MnmE (formerly TrmE)	MNME_ECOLI	*Escherichia coli*	K^+↑, Na^+- K^+ atom in the structure (3)
2	YqeH	YQEH_BACSU	*Bacillus subtilis*	K^+↑, Na^+- (2)
3	TrmE	NP_228080	*Thermotoga maritima*	K^+↑, Na^+- (5)
4	FeoB	YP_139129	*Streptococcus thermophilus*	K^+↑, Na^+- (4)

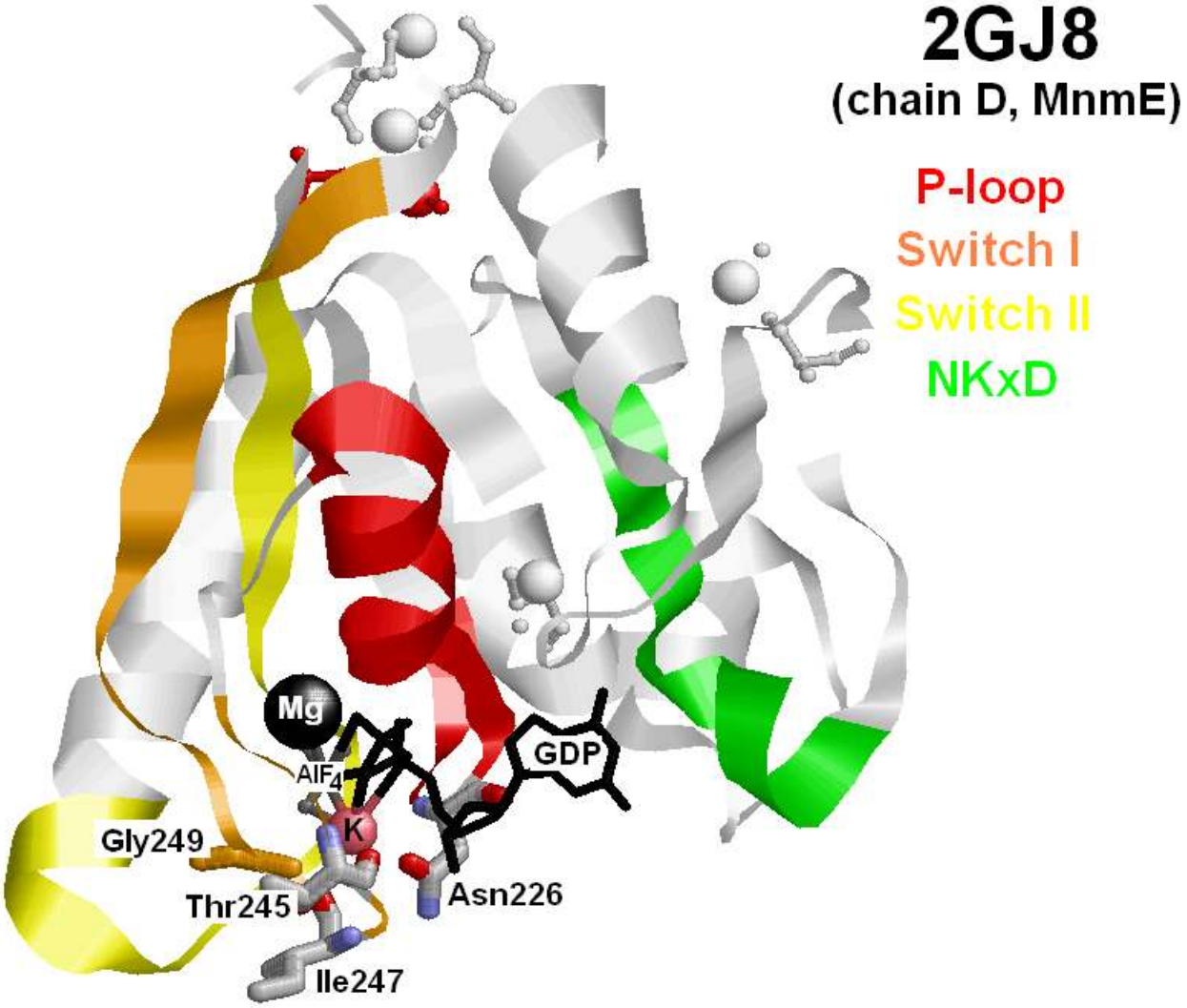

Figure S1. Structure of the MnmE GTPase with the K^+ ion, see ref. (3).

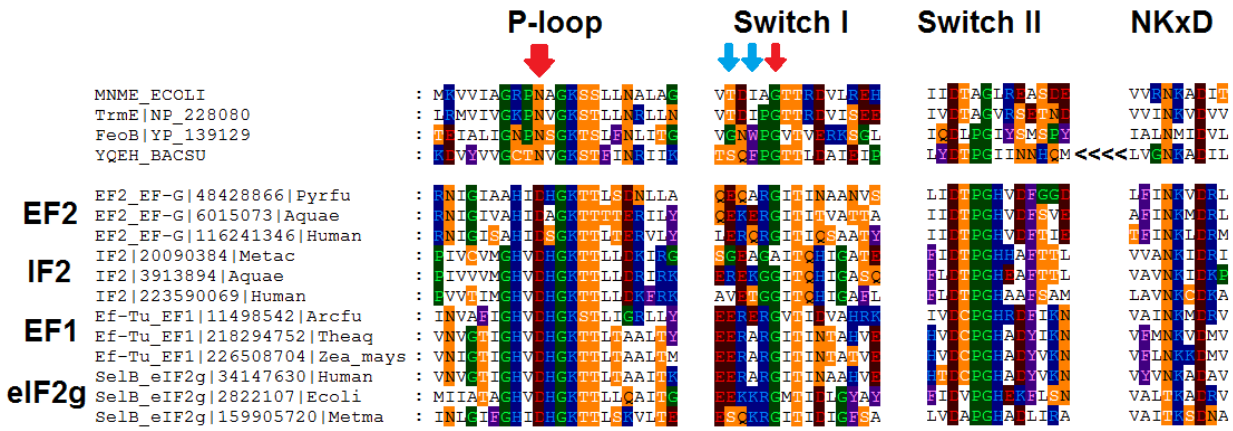

Figure S2. Multiple alignment between potassium-dependent GTPases and the translation factors from Archaea, Bacteria and Eukaryotes. **Bold red arrow** shows the key residue that is important for the binding of the K^+ ion (Asn→Asp in this position in YqeH did not affect the GTPase activity while Asn→Leu or Asn→Gln replacements abolished the enzyme activity (2)). Thin red arrow shows the glycine residue which is not directly involved in binding of the K^+ ion but seems to be important for the flexibility of the protein backbone in this region. Two residues marked with blue arrows participate in binding of the K^+ ion with their backbone oxygen atoms; the exact nature of their side chains is, therefore, of secondary importance. The YqeH protein is circularly permutated and its NKxD motif is located at the N-terminus of the protein (shown by the <<<< sign).

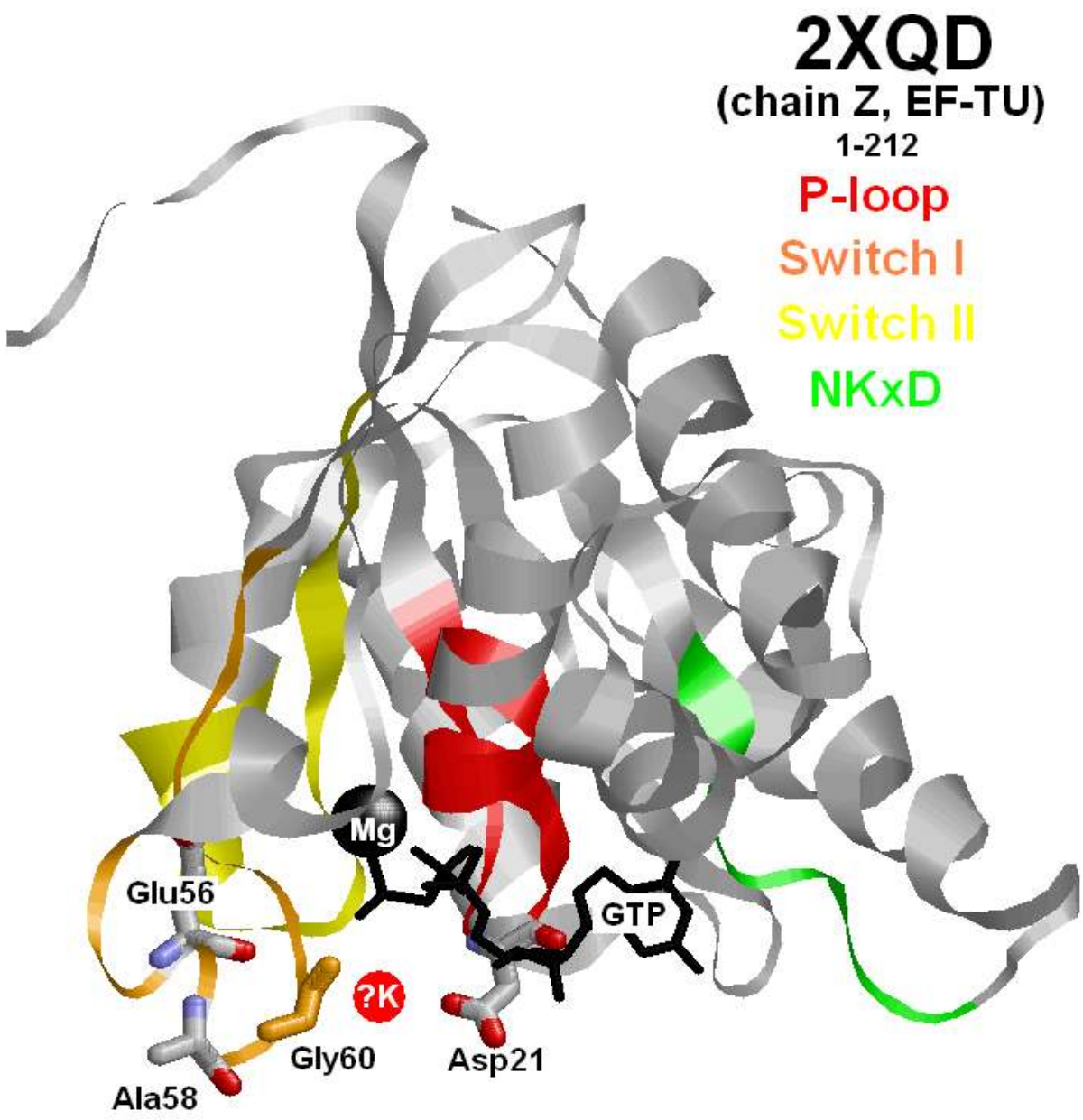

Figure S3. EF-Tu with resolved Switch I region and bound GTP based on a 3.1-Å resolution structure, ref (3). Residues corresponding to those described as K^+-binding are shown in wireframe (compare with **Figure S1**). Although no K^+ ion can be seen in the structure, the arrangement of the residues indicate that a K^+ ion could be present in the position marked with a red dot with a "?" sign. .

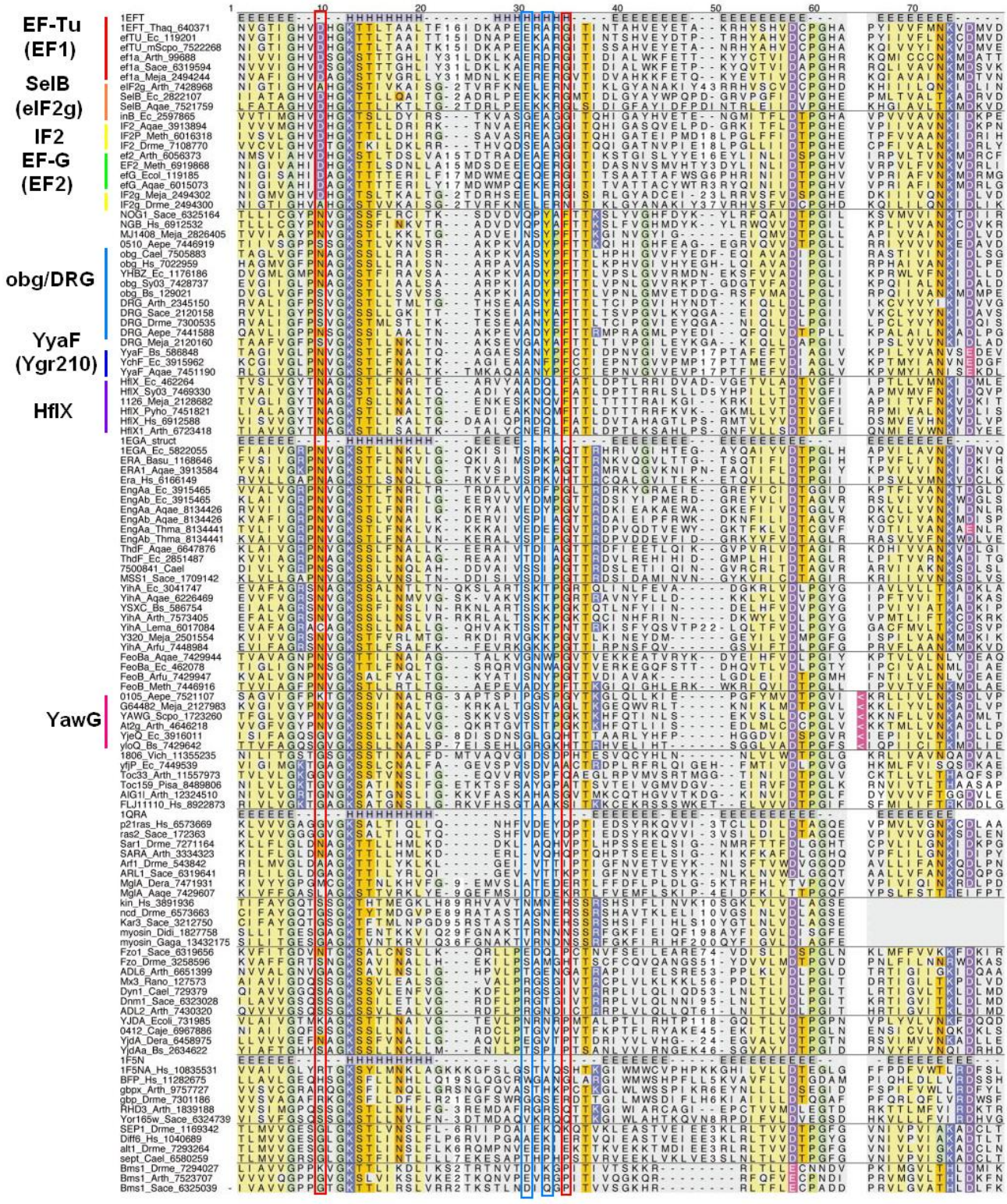

Figure S4. Multiple alignment of GTPases of TRAFAC family from ref. (8). Evolutionarily old protein families are marked at the left. Red and blue rectangles show the same conserved positions as marked by arrows in **Figure S2**.

Table S3. Products of viral hallmark genes (according to (1)) and their association with essential inorganic cations and anions.

(see the caption to Table S1 for the data mining routine)

Protein function	EC number (if available)	Functionally relevant inorganic anions	Functional dependence on monovalent cations	Monovalent cations in at least some structures	Functional dependence on divalent cations	Divalent cations in at least some structures
Jelly-roll capsid protein (JRC) (e.g., VP1 or VP2/VP3)	-	-	-	Na^{+} (1HX6)	-	Ca^{2+} (2W0C, 2VVF, 3FMG), Co^{2+} (3IDE), Hg^{2+} (1M3Y), Mg^{2+} (1LAJ), Zn^{2+} (1JMU)
Superfamily 3 helicase (S3H, SFIII, SF3)	3.6.4.12	phosphate	-	-	Mg^{2+} (2)	Zn^{2+} (1N25, 2H1V, 1SLV), Mg^{2+} (1SLV, 2GXA)
Archaeo-eukaryotic DNA primase	2.7.7.-	pyrophosphate	-	-	Zn^{2+} (3, 4)	Zn^{2+}, Mg^{2+} (1NUI)
UL9-like superfamily 2 helicase (NS3)	3.6.4.12	phosphate	-	-	Mg^{2+} (5)	Mn^{2+} (2JLR)
Rolling-circle replication initiation endonuclease (RCRE)/origin binding protein	-	phosphate	-	-	Mn^{2+} (6)	Zn^{2+} (1M55), Mg^{2+} (1UUT)
Packaging ATPase of the FtsK family	3.6.4.-	phosphate	-	-	Mg^{2+} (7)	absent (1E9R)
ATPase subunit of the terminase	3.6.4.-	phosphate	-	-	Mg^{2+} (8)	absent (2O0H)
RNA-dependent RNA-polymerase (RdRp)/reverse transcriptase (RT)	2.7.7.48		? MC	-	Mg^{2+} (9-11) Mn^{2+} reduces fidelity (11)	Mg^{2+}, Mn^{2+} (2XWY), Zn^{2+} (3OL7)

References

1. Koonin EV, Senkevich TG, & Dolja VV (2006) The ancient Virus World and evolution of cells. *Biology Direct* 1:29.
2. Enemark EJ & Joshua-Tor L (2006) Mechanism of DNA translocation in a replicative hexameric helicase. *Nature* 442:270-275.
3. Pan H & Wigley DB (2000) Structure of the zinc-binding domain of *Bacillus stearothermophilus* DNA primase. *Structure* 8:231-239.
4. Kato M, Ito T, Wagner G, Richardson CC, & Ellenberger T (2003) Modular architecture of the bacteriophage T7 primase couples RNA primer synthesis to DNA synthesis. *Mol Cell* 11:1349-1360.
5. Belon CA & Frick DN (2009) Fuel specificity of the hepatitis C virus NS3 helicase. *J Mol Biol* 388:851-864.

6. Hickman AB, Ronning DR, Kotin RM, & Dyda F (2002) Structural unity among viral origin binding proteins: crystal structure of the nuclease domain of adeno-associated virus Rep. *Mol Cell* 10:327-337.

7. Iyer LM, Makarova KS, Koonin EV, & Aravind L (2004) Comparative genomics of the FtsK-HerA superfamily of pumping ATPases: implications for the origins of chromosome segregation, cell division and viral capsid packaging. *Nucleic Acids Res* 32:5260-5279.

8. Mitchell MS, Matsuzaki S, Imai S, & Rao VB (2002) Sequence analysis of bacteriophage T4 DNA packaging/terminase genes 16 and 17 reveals a common ATPase center in the large subunit of viral terminases. *Nucleic Acids Res* 30:4009-4021.

9. Yu F, Hasebe F, Inoue S, Mathenge EG, & Morita K (2007) Identification and characterization of RNA-dependent RNA polymerase activity in recombinant Japanese encephalitis virus NS5 protein. *Arch Virol* 152:1859-1869.

10. Johnson RB*, et al.* (2000) Specificity and mechanism analysis of hepatitis C virus RNA-dependent RNA polymerase. *Arch Biochem Biophys* 377:129-134.

11. Arnold JJ, Gohara DW, & Cameron CE (2004) Poliovirus RNA-dependent RNA polymerase (3Dpol): pre-steady-state kinetic analysis of ribonucleotide incorporation in the presence of Mn^{2+}. *Biochemistry* 43:5138-5148.

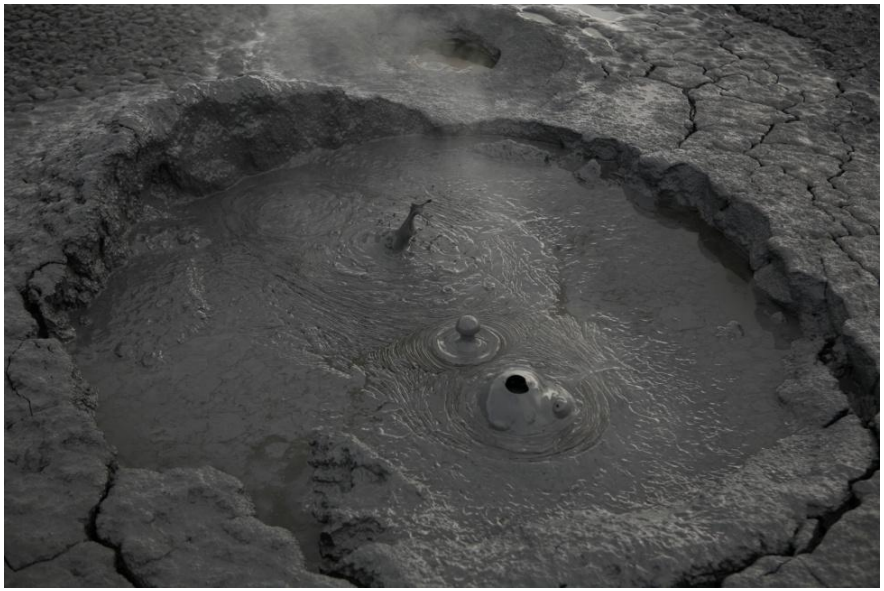

Fig. S5. Boiling, silica-rich pots at Mutnovsky geothermal field, Kamchatka
(Images courtesy of
Dr. Anna S. Karyagina, top,
and Dr. Irina Y. Nikolaeva, bottom)

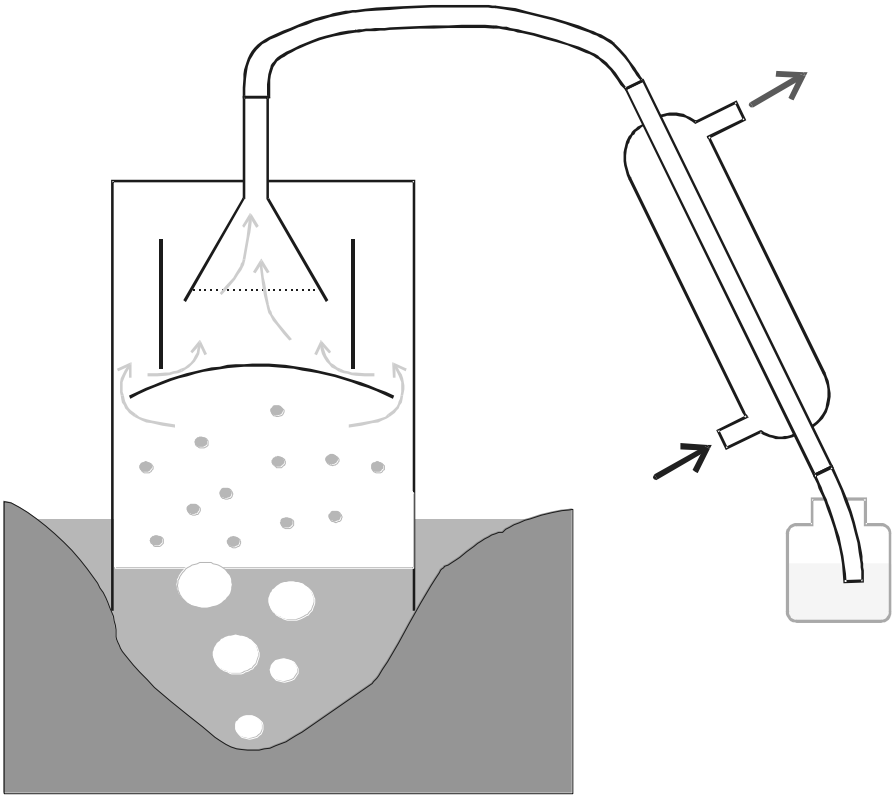

Figure S6. The installation for sampling the thermal springs (see Methods)